
Molecular fingerprint of gilthead seabream physiology in response to pollutant mixtures in the wild

Beauvieux Anaïs ^{5,*}, Fromentin Jean-Marc ¹, Romero Diego ², Couffin Nathan ^{3,4}, Brown Adrien ^{3,4}, Metral Luisa ¹, Bourjea Jerome ¹, Bertile Fabrice ^{3,4}, Schull Quentin ¹

¹ MARBEC, Univ Montpellier, Ifremer, IRD, CNRS, Sète, France

² Toxicology Department, Faculty of Veterinary Medicine, University of Murcia, 30100, Murcia, Spain

³ Université de Strasbourg, CNRS, IPHC UMR 7178, 23 rue du Loess, 67037, Strasbourg Cedex 2, France

⁴ Infrastructure Nationale de Protéomique ProFI, FR2048 CNRS, CEA, Strasbourg, 67087, France

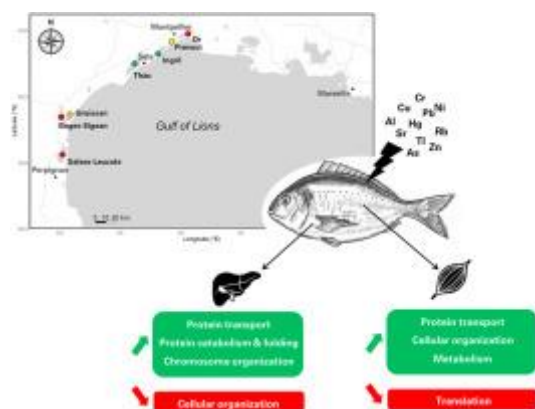
⁵ MARBEC, Univ Montpellier, Ifremer, IRD, CNRS, Sète, France

* Corresponding author : Anaïs Beauvieux, email address : anais.beauvieux@gmail.com

Abstract :

The increase in trace element concentrations in the aquatic environment due to anthropogenic activities, urges the need for their monitoring and potential toxicity, persistence, bioaccumulation, and biomagnification at different trophic levels. Gilthead seabream is a species of commercial importance in the Mediterranean Sea, both for the aquaculture and fisheries sectors, however very little is known about their trace element contamination accumulation and the resulting effect on their health status. In the present study, 135 juveniles were collected from seven coastal lagoons known to be essential nursery areas for this species. We measured seventeen different inorganic contaminants at the individual level in fish muscle (namely Al, As, Be, Bi, Cd, Cr, Cu, Hg, Li, Ni, Pb, Rb, Sb, Sr, Ti, Tl and Zn). Our results revealed the accumulation of multiple trace elements in individuals and distinct contamination signatures between lagoons which might lead to contrasted quality as nurseries for juveniles of numerous ecologically and economically relevant fish species in addition to seabreams. We further evaluated the potential adverse effect of these complex contamination mixtures on the liver (the main organ implicated in the metabolism of xenobiotics) and red muscle (a highly metabolic organ) using a proteomic approach. Alterations in cellular organization pathways and protein transport were detected in both tissues (albeit they were not similarly regulated). Chromosome organization and telomere maintenance in the liver appeared to be affected by contaminant mixture which could increase mortality, age-related disease risk and shorter lifetime expectancy for these juveniles. Red muscle proteome also demonstrated an upregulation of pathways involved in metabolism in response to contamination which raises the issue of potential energy allocation trade-offs between the organisms' main functions such as reproduction and growth. This study provides new insights into the cellular and molecular responses of seabreams to environmental pollution and proposed biomarkers of health effects of trace elements that could serve as a starting point for larger-scale biomonitoring programs.

Graphical abstract



Highlights

► Anthropogenic activities drive aquatic trace element rise, demanding monitoring. ► Little's known about trace element impact on seabream health. ► Seabreams show diverse trace element accumulation in lagoons. ► Contamination affects liver and muscle proteins, impacting health. ► Seabreams face metabolic trade-offs and increased stress due to contamination.

Keywords : Shotgun proteomic, Ecotoxicology, Sparus aurata, Fish health, Lagoon, Cocktail effect

49 Introduction

50 Coastal lagoons are critical transition zones between the marine and continental domains
51 that function as nursery areas and feeding grounds for numerous fish species (Franco et al., 2009;
52 Velasco et al., 2018). However, their proximity to various sources of pollution could reduce their
53 quality as nurseries for juveniles of numerous highly prized fish species (Brusle & Cambrony, 1992;
54 Quignard et al., 1984; Tournois et al., 2017), such as the gilthead seabream *Sparus aurata* (Audouin,
55 1962). In the Gulf of Lions, *S.aurata* performs ontogenetic and trophic migrations between coastal
56 lagoons and the sea (Isnard et al., 2015), related to spawning (Audouin, 1962), settlement and
57 recruitment (Morais et al., 2017). Juveniles that colonise sheltered coastal areas in early winter
58 migrate out to sea the following autumn (Audouin, 1962). However, despite its commercial
59 importance both for the aquaculture and fisheries sectors (Farrugio et al., 1994), very few studies
60 have explored the health effects resulting from contaminant exposure (Isani et al., 2009; Minghetti et
61 al., 2008,2010).

62 Among natural and anthropogenic pollutants, trace elements are present in minute
63 quantities in all environmental compartments. Some of them, such as Cu, Zn and Fe, are essential for
64 animals, including fish, for maintaining basic cellular metabolic processes, in particular through their
65 functional role as co-factors of different enzymes (Wood et al., 2011). However, an excessive
66 concentration of these elements can lead to detrimental effects on a wide range of biological
67 pathways (Gaetke & Chow, 2003). On the other hand, non-essential trace elements, such as Pb, Hg,
68 Cd, As and Ni, can cause toxicity even at very low concentration (Wood et al., 2011). Metals are well-
69 known inducers of oxidative stress in fish, causing an imbalance between the production of oxidative
70 species including reactive oxygen species (ROS) (e.g. H₂O₂, HO·, O⁻², R·, ROO) and cellular antioxidant
71 activity (Halliwell & Gutteridge, 2015). Increased ROS can damage DNA structures and therefore alter
72 the expression patterns of important proteins, different hormones, enzymes, etc. (Javed et al., 2017;
73 Morcillo et al., 2016).

74 Monitoring pollution impacts on living organisms through the use of biomarkers associated
75 with trace element toxicity, such as antioxidant enzymes (Pereira et al., 2013; Williams & Yoshida-
76 Honmachi, 2013), heat shock proteins (HSP, Downs et al., 2006) and metallothioneins (Sakuragui et
77 al., 2013; Williams & Yoshida-Honmachi, 2013) is widespread in environmental and ecotoxicology
78 programs. However, as highlighted by some authors (see e.g., Laviale et al., 2010; Stachowski-
79 Haberkorn et al., 2008), most earlier research lacks environmental realism. The main reason is that
80 past experiments were mainly based on laboratory tests typically performed under controlled
81 conditions, from single-contaminant tests. Yet, wildlife species, including many fish populations,
82 reside and reproduce in an environment where they are continuously and increasingly exposed to
83 complex mixtures of anthropogenic chemicals (especially in coastal areas). These cocktails of
84 contaminants, unlike the effects of single compounds, can have additive, synergistic or antagonistic
85 effects resulting from contaminant interactions (DeLorenzo & Fleming, 2008; Relyea, 2009).
86 Biomarkers based on studies of the effects of single elements may therefore prove useless, as they
87 may respond differently to complex mixtures of pollutants (Celander, 2011). Greater attention must
88 therefore be paid to the toxicity of mixtures for the health of wildlife.

89 The emergence of “omics” tools offers powerful prospects for the analysis of complex,
90 integrated responses to contaminants, and are more sensitive and specific in studying molecular
91 changes in organisms (Benninghoff, 2007; Denslow et al., 2005). Moreover, high throughout shotgun
92 proteomics compared to traditional biochemical methods offers the unique possibility to
93 simultaneously examine, in a single experiment, the thousands of proteins expressed in a specific
94 tissue, which greatly improves our understanding at the molecular level (López-Pedrouso et al., 2020;
95 Sanchez et al., 2011). Furthermore, it presents a unique opportunity to identify few relevant
96 biomarkers, which could be then used to develop more effective monitoring programs for assessing
97 the impact of pollutants on marine species (Apraiz et al., 2006; Benninghoff, 2007).

98 The present study assessed *in-situ* inorganic pollutant contamination in juveniles of gilthead
99 seabreams in the Gulf of Lion (NW Mediterranean Sea) and the impact of these cocktails of
100 contaminants on individual health using a proteomic approach. Our objectives were: 1) to assess
101 trace element contamination patterns in wild *S.aurata* juveniles across 7 lagoons of the Gulf of Lion,
102 2) to investigate their impact on the proteome of the liver (the main organ implicated in the
103 metabolism of xenobiotics) and red muscle (a highly metabolic organ), in order to unravel the
104 possible adverse effects of accumulated pollutants on individual's health and to identify for both
105 tissues a few potential biomarkers that could serve as valuable tools for long-term monitoring of
106 gilthead seabream health.

107 Materials and Methods

108 Study sites and sampling

109 In this study conducted in the Gulf of Lions (Northwestern Mediterranean Sea), 135 juveniles
110 of *Sparus aurata* were collected from seven coastal lagoons known to be essential nursery areas for
111 this species (Tournois et al., 2017, ESM1). Specimens were collected in October-November 2021
112 using traditional passive fishing gear, called "capechade", composed of a pound net and several fyke
113 nets, commonly used by fishermen in lagoons. Among those 135 juvenile individuals, between 17
114 and 20 fishes were sampled in each lagoon and were measured (total length TL, in mm) and weighed
115 (total mass M, in g). Their body condition was estimated based on the Fulton's index K (Rätz & Lloret,
116 2003), commonly used as an indicator of general well-being and calculated as follows:

$$K = 10^5 M / TL^3$$

117 where M is the total wet mass in g and TL the total length in mm.

118 Liver and red muscle (taken on the midline of the flank) were removed, snap-frozen in liquid
119 nitrogen and stored at -80 °C for proteomic analysis. White muscle of left fish sides taken from the
120 epaxial mass was removed and stored at -40°C for trace element analysis. Red muscle was cleanly
121 separated from white muscle by scraping the lateral skin stripped from the animal.

122 Trace-element analysis

123 All samples were lyophilized using the freeze dryer Lyovac GT4 (Leybold, Cologne, Germany).
124 For Al, As, Be, Bi, Cd, Cr, Cu, Li, Ni, Pb, Rb, Sb, Sr, Ti, Tl and Zn determination, the samples underwent
125 a pre-treatment process where 0.5 grams of each muscle sample were subjected to acid digestion
126 using 4 mL of HNO₃ (69%) and 1 mL of H₂O₂ (33%) in special Teflon reaction tubes within a
127 microwave digestion system (UltraClave-Microwave Milestone®) for 20 minutes at 220 °C, and then
128 diluted to 10 mL with double deionized water (Milli-Q). Samples were analyzed using inductively
129 coupled plasma optical emission spectrometry (ICP-OES, ICAP 6500 Duo, Thermo) to determine the
130 levels of this elements. The detection limit was 0.001 mg/kg. Each sample was read in duplicate and
131 averaged. Based on UNE-EN ISO reference 11885, multi-element calibration standards (SCP Science,
132 in 4% nitric acid) were assembled with different concentrations of inorganic elements. For
133 calibration, see (Romero et al., 2020).

134 Total mercury (Hg) content was measured using an atomic absorption spectrometer AMA254
135 Advanced Mercury Analyzer (Leco) without pre-treating or pre-concentrating the samples
136 (wavelength = 253.65 nm, detection limit (DL) = 0.003 µg.g⁻¹). The recovery rate for reference
137 materials (Mercury ICP Standard 1000 mg L⁻¹ Hg, Merck) was above 95%.

138 Quantitative proteomic analysis

139 Proteomic analyses of liver and red muscle were conducted as two separate experiments on
140 a subsample of 31 individuals selected based on their inorganic contamination levels in white muscle,
141 so that one half of juveniles displayed the lowest trace element load (n = 15) and the other half the
142 highest (n = 16) (see Statistical analysis section for further details on individuals 'selection). The
143 process of sample preparation, nanoLC-MS/MS analysis, and mass spectrometry data analysis is
144 described in detail in ESM2. The procedure involved protein extraction and electrophoresis using
145 SDS-PAGE, followed by in-gel digestion with trypsin (Promega, Madison, WI, USA). The resulting
146 peptides were extracted and analyzed using a nanoUPLC-system (nano-Acquity, Waters, Milford, MA,
147 USA) coupled to a quadrupole-Orbitrap hybrid mass spectrometer (Q-Exactive HF-X, Thermo

148 Scientific, San Jose, CA, USA), controlled by XCalibur software (v4.0.27.9; Thermo Fisher Scientific).
149 The Q-Exactive HF-X was operated using a data-dependent acquisition (DDA) strategy by selecting
150 the Top-20 most intense ions in MS1 for fragmentation in MS2. MS raw data processing was
151 performed in MaxQuant (v2.0.3.1) (Cox et al., 2014), using Andromeda algorithm to search peaklists
152 against a protein database containing the 69,200 protein sequences from the *S. aurata* UniprotKB
153 proteome (TaxID: 8175; Reference proteome ID: UP000472265; July 2022). Only the proteins
154 identified with at least two unique peptides were retained. Protein quantification was performed
155 using unique peptides only via the MaxLFQ option implemented in MaxQuant (Cox et al., 2014). The
156 mass spectrometry proteomics data have been deposited to the ProteomeXchange Consortium via
157 the PRIDE (Perez-Riverol et al., 2019) partner repository with the dataset identifiers PXD037424
158 (liver) and PXD037412 (red muscle). During the analysis, protein extraction was unsatisfactory for
159 one red muscle sample, which was subsequently removed. QC-related measurements indicated
160 stable performances of the analysis system all along the two experiments, with median coefficients
161 of variation (CV) of 0.41% (liver) and 1.2% (red muscle) for retention times of iRT peptides over
162 all injections. Median CVs of only 8.8% (liver) and 11.1% (red muscle) were obtained for LFQ values of
163 the proteins quantified from the repeated injections of reference samples.

164 Protein functional annotation

165 In order to analyse our proteomic data from a functional point of view, we examined the
166 functional annotations of proteins listed by the AMIGO consortium (Gene Ontology, GO;
167 <http://geneontology.org/>). However, only a handful of *S. aurata* proteins are annotated in GO
168 databases. We therefore took advantage of the crucial evolutionary position of the spotted gar
169 (*Lepisosteus oculatus*) between teleost fishes and humans, which creates a very valuable bridge
170 between their genomes (Braasch et al., 2016) and of the fact that gar proteins are well annotated in
171 GO databases. We began by searching *L. oculatus* sequences (UniprotKB, 22,463 protein entries;
172 September 2022) for proteins homologous to *S. aurata* proteins using BLAST searches (FASTA v36.1.4
173 program; downloaded from http://fasta.bioch.virginia.edu/fasta_www2/fasta_down.shtml), and
174 only the top BLAST hit for each protein was retained. From *L. oculatus* protein sequences, the same
175 strategy was employed to search for human homologous proteins (TaxID: 9606; Reference proteome
176 accessed in September 2022). The relevance of the match between homologous proteins was checked
177 manually and only 146 of 3104 matches could not be validated. An automatic extraction of GO
178 annotations was then performed using the MSDA software (Carapito et al., 2014).

179 Statistical analysis

180 Element concentrations below LODs (0.001 mg/kg) were set to $\text{LOD}/\sqrt{2}$ as suggested as the
181 best substitution method by Verbovsek (2011). Analyses comparing trace elements contamination
182 patterns included only elements that were detected in at least 50% of individuals out of the 135
183 collected. In order to detect possible relationships between contamination and fish body size, we
184 used a linear model (LM) between each contaminant concentration and total length. Normality and
185 homoscedasticity of the residuals were verified using the Shapiro's and Levene's tests respectively.
186 When residuals distribution did not follow a normal distribution, a Box-Cox-based transformation was
187 applied prior to model fitting. If necessary ($P < 0.05$), size-corrected contaminant was defined as back-
188 transform residuals of the regression model.

189 To investigate relationships between contaminants within and between lagoons, we ran
190 Principal Component Analysis (PCA) on trace element concentrations (size-corrected when required)
191 of the 135 individuals. Furthermore, radar plots of the seven sampling sites (lagoons) were drawn
192 based on trace element concentrations.

193 In the following proteomic approach, we analyzed a subset of 31 individuals who exhibited
194 the most distinct contamination profiles. This selection process involved assigning ranks to
195 seabreams (from all lagoons) based on the level of each contaminant detected. The ranking ranged
196 from 1 (indicating the lowest contamination level) to 135 (representing the highest contamination
197 level). The individuals were then chosen based on the total sum of these ranks. Consequently, we
198 identified two groups, one comprising 15 seabreams with the lowest contamination levels, and the
199 other consisting of 16 seabreams with the highest contamination levels. Then, PCA using the 31
200 individuals as objects and the 14 contaminants as descriptors was run, using a correlation matrix.
201 PCA axes (PC1, PC2, PC3) were then retained as the three main contaminant mixtures (or cocktails of
202 contaminants) found in seabreams. These three contaminant mixtures were used in further analyses.

203 Prior to statistical analyses, the proteomic datasets were filtered to keep only proteins that
204 were expressed in at least 70% of individuals in each contamination group leaving 2742 (out of 3104)
205 and 1018 (out of 1218) expressed proteins in the liver and red muscle, respectively. Two and three
206 individuals were removed due to a high number of missing values for liver and muscle proteomic
207 analysis respectively. Missing values were imputed for each contamination group based on random
208 forest method. Previous studies have shown that this method exhibits strong performance and is
209 particularly well-suited for label-free proteomic studies, where the underlying reasons for missing
210 data are not fully understood (Jin et al., 2021; Kokla et al., 2019). The variance stabilization
211 normalization (vs_n) method was used to normalize the protein intensities. This method
212 demonstrated good performance in evaluating differential expression statistics. (Välikangas et al.,
213 2018). The aim of performing VSN normalization is to standardize the scale of samples. This is

214 accomplished by initially removing any variance that may have arisen from systematic experimental
215 factors, followed by the application of a generalized log₂ transformation.

216 Statistical analyses were performed with the statistical open source R software v.4.1.1 (R
217 Core Team 2021) using the packages “FactoMineR” v.2.4 (Lê et al., 2008), “factoextra” v.1.0.7
218 (Kassambara & Mundt, 2020), “missForest” V.1.5 (Stekhoven & Bühlmann, 2012) and “DEP” V.1.16.0
219 (Zhang et al., 2018).

220 Co-expression network and enrichment analysis

221 *Gene co-expression network and identification of hub proteins*

222 Weighted gene co-expression network analysis implemented in the WGCNA R package
223 (Langfelder & Horvath, 2008) was used for both tissues (liver and red muscle) to identify groups,
224 hereafter named “modules”, of proteins whose expression significantly correlates with the three
225 retained trace element mixtures. First, a signed adjacency matrix for all pairs of proteins was
226 constructed using the spearman correlation raised to the power (beta) of six and four to approximate
227 a scale-free network for liver and red muscle, respectively. The adjacency matrix was then
228 transformed into a topological overlap dissimilarity matrix and a combination of hierarchical
229 clustering. A dynamic tree-cutting algorithm was used to first define and then merge co-expressed
230 modules of proteins. Proteins outside any modules (indicating low co-expression) were gathered in a
231 “grey module”. The module's eigengene (i.e. first axis of a principal component analysis conducted
232 on the expression of all proteins of a given module) summarizes the expression of all proteins in that
233 module. Then, we investigated whether each module's eigengene was correlated with each trace
234 element mixtures (PC1, PC2 and PC3), using spearman correlation. Modules with a significant
235 ($P < 0.05$) spearman correlation of at least 0.4 were retained for further analysis. Positive and
236 negative relationships reflect the up- and down-regulation of the module with increasing
237 contaminant concentration, respectively. To explore the functional and physiological mechanisms
238 associated with each module, we performed functional enrichment analyses.

239 *Functional enrichment analysis and pathway network*

240 For both tissues, enrichment analysis (biological process and cellular component) of the
241 proteins constituting each module was performed using Fisher's exact test using the 'GO_MWU'
242 package particularly suitable for non-model organisms (https://github.com/z0on/GO_MWU) (Dixon
243 et al., 2015). It allows to determine the functional significance of the identified modules. Enriched GO
244 terms are displayed in a dendrogram plot with distances between terms reflecting the number of
245 shared proteins. Additionally, we assessed the Spearman correlation between each protein and the
246 trace element mixtures (PCA axes) to infer "gene significance" (GS). These GS relationships were
247 compiled within a circle plot for each enriched pathway of the module, focusing on the top 10
248 enriched biological process terms (GO terms). These plots highlight the up- or down-regulation of the
249 proteins and pathways in response to the three trace element mixtures.

250 *Network visualization*

251 ClueGO was used to illustrate overrepresented Gene Ontology. ClueGO is a Cytoscape plug-in
252 that visualizes the non-redundant biological terms for large numbers of proteins and integrates the
253 GO terms to create a GO/pathway network (Bindea et al., 2009). A network for each tissue was made
254 in order to have a better visualization of the pathways impacted by the three trace element mixtures.

255 *Hubproteins identification*

256 Finally, for each module, GS was correlated with module membership (MM; spearman
257 correlation of protein intensity *versus* the module eigengene) to identify proteins that show the
258 highest degree of connectivity within a module and with the considered trace element mixture (hub
259 proteins). The top 5 proteins with simultaneously the highest module membership and gene
260 significance (rank sum) were selected as hub protein of each module. Due to their central position in
261 the network, hub proteins are expected to play important biological roles within their module and
262 are considered as potential biomarkers.

263 *Functional Comparison between tissues*

264 For each trace element mixture, the similarity in functional response between tissues was
265 compared by plotting their respective GO term delta ranks against each other. A GO term delta rank
266 corresponds to the difference between the mean rank (based on GS values) of annotated proteins it
267 contains vs the mean ranks of all the protein not included. Positive and negative delta ranks indicate
268 the GO term tends toward upregulation and downregulation, respectively. The strength of the
269 relationship reflects the similarity between enrichments. It is important to note that these plots do
270 not represent a formal statistical test, as the data points (gene ontology categories) are not
271 independent. Indeed, they often encompass overlapping sets of proteins, nonetheless it allows
272 identifying functional similarity or dissimilarity between functional enrichments.

273 Results

274 Contamination profiles

275 After selection of contaminants detected (>LOD) in at least 50% of individuals (*i.e.* 68
276 individuals), we retained 14 trace elements in white muscle (Al, As, Cd, Cu, Cr, Hg, Li, Ni, Pb, Rb, Sr, Ti,
277 Tl and Zn, ESM3). Only six exhibited significant but low correlation with fish total length and were
278 size-corrected (*i.e.*, aluminium, arsenic, lithium, strontium, thallium and zinc). While aluminum had
279 positive relation with fish size ($R^2 = 0.03$, $P < 0.05$), arsenic ($R^2 = 0.24$, $P < 0.001$), lithium ($R^2 = 0.08$,
280 $P < 0.001$), strontium ($R^2 = 0.07$, $P < 0.01$), thallium ($R^2 = 0.07$, $P < 0.01$) and zinc ($R^2 = 0.05$, $P < 0.01$)
281 displayed a negative association.

282 The first three axes of PCA performed on the 135 individuals as objects and contaminants
283 concentration as descriptors reflected 20.6%, 14.5% and 11% of the total variance, respectively
284 (ESM4). Cu, Cr, Ni, Al, Tl; Rb were all positively loaded on PC1. Rb, Tl and As were significantly and
285 positively loaded to PC2 in opposition to Pb, Al and Ti. Sr and Cr were negatively loaded on PC3 in
286 opposition to Zn, Ti, As and Pb (ESM4). The projection of the seven lagoons within the same PCA
287 highlighted a large overlap of the contamination between lagoons. Considering trace element levels
288 along the PC1 axis, individuals from Prevost and Ingril lagoons displayed low contamination

289 compared to Salses-Leucate, Or and Bages-Sigean lagoons. Notably Bages-Sigean lagoon revealed a
290 high variance dispersion (inter-individual variability, Figure 1). Moreover, radar plots were used to
291 visually compare the contamination profile across sampling sites (ESM5). The radar plots for the
292 different lagoons varied markedly. Indeed, Ingril and Prevost lagoons displayed generally low
293 concentrations of all elements, except for mercury, which exhibited the highest level in the Prevost
294 lagoon (ESM5e). Seabreams captured in Bages-Sigean and Salses-Leucates presented the highest
295 concentration in 5 elements (Al, Cu, Ti, Sr, Pb; ESM5a and f). High levels of Cr, Rb, Sr and Nickel were
296 found in the Or lagoon (ESM5d). The radar plot of the Thau contamination showed low to medium
297 concentrations for all elements (ESM5g). Finally, Gruissan revealed the greatest concentration in Zn
298 and high levels of As (ESM5b).

299 The first 3 principal components of the PCA ran on the 31 individuals selected for proteomic
300 analysis, reflected 28%, 17.4% and 10.5% of the total variance respectively (ESM6). PC1 clearly
301 separated the 2 groups of individuals previously selected (high contamination vs low contamination).
302 and reflected higher contamination in Al, Cu, Sr, Pb, Ni, Cr, Tl and Ti. PC2 (contaminant mixture 2)
303 reflected higher contamination to Rb, Tl, As and Zn and lower contamination to Pb while PC3
304 (contaminant mixture 3) reflected higher contamination to Hg, Zn, Ni and (in a lower proportion) Pb
305 and a lower contamination to Sr. The three PCs independently reflected trace element
306 mixtures/profiles as resumed in Table 1.

307 [Physiological response to inorganic contamination exposure](#)

308 The three contaminant mixtures based on the PCA with 31 individuals displayed no
309 significant correlation with individual body condition. Therefore, we further investigated the impact
310 of trace element contamination at the proteome level on two central organs in fish (the liver and the
311 red muscle) using a co-expression network analysis.

312 [Liver proteome](#)

313 After the definition of the protein network, we applied a dynamic clustering method
314 implemented in WGCNA to identify modules of highly correlated proteins. We identified 18 different

315 modules encompassing a total of 2742 proteins. We then examined the relationship between
316 expression modules and the three contaminant mixtures to assess contaminant exposure
317 consequences on individual health. Three co-expressed modules exhibited significant correlation
318 ($P < 0.05$) with either mixtures 1, 2 or 3 (Figure 3a and 4).

319 Mixture 1 and Mixture 3 showed positive relationship with the pink and turquoise modules,
320 respectively, while Mixture 2 was negatively correlated to the magenta module. A positive
321 relationship highlights an overexpression of the proteins in the module with increasing
322 contamination, while a negative relationship reflects an underexpression of the proteins in the
323 module with increasing contamination. In detail, pathway enrichment within the pink module
324 included “vesicle transport” with proteins overexpression with increasing contamination with
325 mixture 1 (Al, Cu, Sr, Pb, Ni, Cr, Tl and Ti, ESM7a and c). Proteins from this module were mainly
326 located in nuclear pores (ESM7b). On the contrary, the negative correlation of the Magenta module
327 with increasing contamination with mixture 2 (Rb, Tl, As, Zn and - Pb) indicated a downregulation of
328 the 52 enriched pathways mainly related to cytoskeleton/cellular organization (ESM8a and c).
329 Accordingly, the GO cellular component analysis highlighted that these proteins were mainly
330 involved in the cytoskeleton (ESM8b). Finally, the positive relationship with the turquoise module
331 revealed an up-regulation of proteins mainly involved in protein catabolism, chromosome and
332 telomere organization and protein folding (ESM9a and c) with increasing levels of Hg, Zn, Ni and Pb
333 and decreasing Sr (mixture 3). As for the cellular component involved, proteins were essentially part
334 of protein complexes involved in protein metabolism (*e.g.* proteasome complex, chaperone complex)
335 and microtubules (ESM9b).

336 To identify potential biomarkers, hub proteins (*i.e.*, the top 5 proteins with the highest GS
337 and MM) were selected for each module (see ESM10). Within the pink module (positively linked to
338 mixture 1), hub proteins were implicated in protein transport and/or localization (ESM10). Notably
339 one of them (Dynamin 1-like protein) is also involved in necrosis pathways. Within the Magenta

340 module (negatively linked to mixture 2), three hub proteins were involved in metabolism (pyruvate
341 or phospholipid processes) or cellular structure. We noted that one of these proteins (gelsolin,
342 ESM10) is also involved in apoptosis. Finally, hubproteins for the turquoise module (responding to
343 mixture 3) were associated with multiple functions such as DNA damage repair, protein folding,
344 response to ROS and oxygen homeostasis (ESM10).

345 Muscle proteome

346 A total of five modules including blue (159 proteins), brown (119 proteins), turquoise (594
347 proteins), green (48 proteins), yellow (95 proteins) and grey (3 proteins) were obtained from WGCNA
348 analysis of the red muscle proteome. Only two modules (turquoise and green) correlated significantly
349 with contaminant mixtures 1 and 2 (Figure 3b and 5).

350 Turquoise module correlated positively with mixture 1 ($P < 0.01$) and mixture 2 ($P < 0.05$) and
351 was enriched in 52 pathways mainly involved in metabolism (carbohydrate metabolism, protein
352 metabolism/translation and energy metabolism), cellular structure and muscle organization
353 (ESM11a, c and d). All GO terms were upregulated with increasing level of contaminants of mixture 1
354 (including Al, Cu, Sr, Pb, Ni, Cr, Tl and Ti) and mixture 2 (increasing Rb, Tl, As, Zn and decreasing Pb).
355 GO cellular component analysis revealed no significant enrichment (ESM11b). Green module
356 consisted of fewer proteins (48) and was enriched in protein biosynthesis/translation pathways
357 which were all downregulated with increasing level of mixture 2 (ESM12a and c). Here again, no
358 cellular component was significantly enriched (ESM12b).

359 Hub proteins identified within the turquoise module were all involved in carbohydrate
360 metabolism except the “ryanodine receptor 1” (RYR1, ESM13) being involved in muscle contraction.
361 4 out of five potential biomarkers of contamination mixture 2 (green module) were ribosomal
362 protein involved in protein translation apart from a subunit of tubulin implicated in cellular structure
363 (ESM13).

364 Comparison of liver vs red muscle proteome response

365 Comparison of the delta-rank values obtained from GO enrichment analysis for both tissues in
366 regard to mixture 1 revealed no significant correlation ($P > 0.05$, ESM14). However, enrichment in
367 regard to mixture 2 and 3 displayed low but significant correlations ($cor = -0.16$, $P < 0.001$ and $cor = -$
368 0.12 , $P < 0.01$ for mixtures 2 and 3, respectively). This highlights that similar processes appear involved
369 in response to these two contaminant mixtures, albeit with opposite responses for the two tissues.

370 Discussion

371 The increase in trace element concentrations in the aquatic environment due to
372 anthropogenic activities highlights the importance for a better monitoring of their potential chronic
373 persistence, bioaccumulation, biomagnification and toxicity at different trophic levels (Marengo et
374 al., 2018). We found evidence for the accumulation of multiple elements in gilthead seabreams from
375 seven different lagoons with specific contamination signatures. Physiological responses that involved
376 cellular organization pathways and protein transport were detected in both the liver and red muscle
377 (albeit they were not similarly regulated). We also highlighted processes such as metabolism and
378 translation that were specifically affected in red muscle. From our results, we propose hubproteins as
379 biomarkers of health effects of metal stress that could serve as a starting point for larger-scale
380 biomonitoring programs.

381 Contamination profile

382 Fish size is often recognized important in determining the rate of physiological processes that
383 influence uptake, distribution and elimination of inorganic contaminants (Canli & Atli, 2003). Our
384 analysis revealed that 6 out of 14 contaminating elements showed significant correlation with size,
385 highlighting that mean concentration of trace elements in muscle were not systematically linked to
386 fish length. The absence of relationship for essential trace elements likely indicates that fish regulate
387 some element at a concentration required for efficient metabolic activities (Canli & Atli, 2003). When
388 correlation occurred, most relationships with size were negative except for aluminium, which is in
389 agreement with results found by Endo et al. (2008). Previous studies have already shown inter-

390 specific differences in trace element dynamic (e.g. Gobert et al., 2017; Mille et al., 2018). This may
391 result from a higher metabolic activity in fast-growing young individuals, or through a higher
392 excretion rate and/or dilution of metal burden with growth (Eisler, 2010). Another explanation could
393 be a change in diet with growth, where smaller individuals specialize in certain prey species or
394 foraging areas that are more contaminated. More interestingly, no relationship between mercury
395 concentration and total length were found despite being known to bioaccumulate (Storelli et al.,
396 2007). Similar results were found for one year old juveniles of the Mediterranean sardines which
397 suggests that when focusing at one age-class, the variability in size within necessarily remain low and
398 so further investigating on several age-classes are needed to reveal complex bio-accumulation
399 patterns.

400 Despite high inter-individual variability within sites suggesting variable accumulation among
401 individuals, our results clearly showed differences in the exposure to trace elements among the
402 seven coastal lagoons. Similar results have been reported by Tournois et al. (2017), who highlighted
403 clear differences among lagoons in the relative level of multiple trace elements in otolith of gilthead
404 seabream juveniles. As fish take up trace elements through the gills, digestive tract, and body surface
405 (Kamunde et al., 2002; Tao et al., 2001) comparison with metal contamination of other matrixes in
406 the close environment of seabreams such as sediment, water and mussel (preys of gilthead
407 seabreams) could help to explain such accumulation differences between lagoons and individuals
408 (Andral & Tomasino, 2010; Grouhel et al., 2018; Munaron et al., 2013). Interestingly, contamination
409 in fish muscle seemed related to prey contamination for Gruissan, Prevost and to a lesser extent
410 Bages-Sigean lagoons (ESM15). The findings align with the well-known phenomenon of
411 biomagnification in aquatic food webs, where trace elements tend to accumulate at higher trophic
412 levels (Fey et al., 2019). However, the contamination in multiple trace elements for Salses-Leucate,
413 Bages-Sigean and Or lagoons could not be explained by contamination in other environmental
414 matrices mostly because some trace elements measured in this study (aluminium, rubidium,
415 thallium, lithium, titanium and strontium) were not monitored in sediment, water nor biota.

416 Moreover, either weak or no relations were found between muscle trace element concentration and
417 water or sediment contamination (ESM15), even for Ni and Zn that are described as elements with
418 the highest partial correlation with muscle contamination load (Pyle et al., 2005). This observation
419 supports the understanding that in low-contaminated waters, the primary mechanism for metal
420 uptake in fish occurs predominantly through feeding. (Farkas et al., 2003). These patterns underlined
421 that accumulation of trace elements in fish does not directly reflect their simple concentration in the
422 surrounding environment because as it is also affected by environmental factors (pH, organic matter
423 content temperature etc.), species biology and the physico-chemical properties of the contaminants
424 (speciation, solubility, complexation etc., P Cresson et al., 2015). Thus, assessing a site-specific
425 contamination patterns requires a good knowledge of all the environmental and biological factors as
426 well as their potential interactions, which can lead to high inter-individual variance within each site
427 (Schull et al., 2023).

428 In general terms, trace metal concentrations reported in our study were within the ranges
429 reported in Mediterranean and Black Sea seabream populations from Algeria, Croatia, France,
430 Greece, Italy, Spain and Turkey, except for aluminium and lithium (ESM16). In our study, average Al
431 level was 1.3 to 8 times higher than those reported in the literature (Bouchoucha et al., 2019; Guérin
432 et al., 2011; Marengo et al., 2018). Similarly, Li concentrations were 3 times higher than those
433 described in Guérin et al. (2011) and Marengo et al. (2018) although the former one measured Li
434 levels in only 4 individuals. However, the most striking observation was the lack of data for multiple
435 elements including Rb, Sr, Ti and Tl (but see Bouchoucha et al., 2019; Guérin et al., 2011). This is
436 partially explained by the absence of regulatory limits for those elements in fish muscle (along with
437 Cr and Ni), despite their increasing use in multiple area (industrial, agriculture, high-tech and
438 medication industries) and their toxicity for organisms (Aslam & Yousafzai, 2017; Authman, 2011;
439 Blewett & Leonard, 2017; Exley et al., 1991; Genchi et al., 2021; Kumari et al., 2017). Nonetheless,
440 metal concentrations are expressed, in literature, either per unit of wet (ww) or dry (dw) tissue
441 weight as it was the case in this study. A lack of standardized levels of elemental concentrations

442 limits the comparability of studies (Jovičić et al., 2015). Cresson et al. (2017) demonstrated that the
443 theoretical wet:dry ratio of 5 traditionally used was not valid for all species, and that conversion
444 values were ranging from 3.6 to 5.5 depending on the species. In our case, we used 4.31 as factor as
445 Minganti et al. (2010) used for *Sparus aurata*.

446 The European regulation has set contamination thresholds for only three specific inorganic
447 trace elements, namely Pb (lead), Cd (cadmium), and Hg (mercury), while some countries (for
448 instance Turkey and Greece) have encompassed a larger set of contaminants (for a review see
449 Guerra-García et al. 2023). Notably, trace element loads measured in seabreams for this study
450 remained below the threshold values in fish for human consumption provided by most international
451 regulations, with the exception of arsenic (As) which exceeded these limits. These results urge
452 further efforts by European commission and other institutions to establish health limits in fish,
453 especially for As.

454 Contaminant mixture and their physiological effects

455 In the light of our results, it appears that juvenile seabream, regardless of the environment in
456 which they are living, are exposed to different mixtures of contaminants, which is in line with
457 previous results concerning the same areas in older fishes (Schull et al., 2023). According to the PCA
458 on metal contamination of the 31 individuals selected for proteomic analysis, three different
459 contamination profiles were identified (Table 1). One of the major interests of using PCs as a
460 continuous proxy for general inorganic contamination level is to work along contamination gradient
461 instead of categorial contamination. However, a limit of this approach is when some elements level
462 increases, others decreases as it the case for PC2 and PC3, preventing specific contaminant effects
463 from being identified.

464 Liver proteome response

465 Considering the liver proteome, each mixture elicited a specific physiological response,
466 highlighted by the fact that each PC correlated with only one protein module. Mixture 1 (Al, Cu, Sr,
467 Pb, Ni, Cr, Tl and Ti) impacted vesicle protein transport known to be key for protein localization and

468 function. Indeed, protein function depend on their subcellular localization, with each cell
469 compartment offering different chemical environments (e.g. pH and redox conditions) and different
470 potential interaction partners or substrates (Lundberg & Borner, 2019). Tight regulation of protein
471 subcellular localization is hence an important layer of control over cell physiology (Bauer et al., 2015)
472 and its up-regulation, appears to be a potential response to metal stress. More precisely, mixture 1
473 seemed to particularly affect proteins located in nuclear pores. The nuclear pore complex is the
474 major gateway to the nucleus and regulates nucleocytoplasmic transport, which is central to
475 processes including transcriptional regulation and cell cycle control (Paci et al., 2021). This result may
476 represent mechanisms developed by cells to defend against trace element toxicity , either through a
477 direct response to the contaminant or through an indirect process.

478 Furthermore, mixture 2 (PC2) including contamination in Rb, Tl, As, Zn and -Pb impacted
479 specifically hepatocyte structure and organization with enrichment in pathways, such as regulation of
480 actin filament polymerisation. Actins are abundant cytoskeleton proteins (involved in microfilaments)
481 with an important function in intracellular transport, cell organization and motility processes
482 (Goodson & Hawse, 2002). Another protein particularly affected by mixture 2 was the gelsolin
483 protein involved in cellular structure (downregulated, ESM10). This protein was previously identified
484 in oysters as responsive to inorganic contamination as well (Li et al., 2020) and was linked to
485 inhibition of cellular apoptosis (Koya et al., 2000), which made it a great candidate as a biomarker of
486 metal contamination. Furthermore, dysregulation of cytoskeleton affects many cellular mechanisms,
487 ranging from cell motility to the maintenance of cell shape and polarity. This is in line with the
488 significant downregulation in the pathway involved in establishment and maintenance in cell
489 polarity. Cell polarity plays a particularly important role in hepatocyte function such as the
490 sustainment of two concurrent flow systems (bile and sinusoidal blood components) and in liver
491 regeneration (Treyer & Müsch, 2013). Contaminant effects on cellular integrity were also observed
492 in literature at the tissue level with liver histopathological damage, including hyperemia and
493 leukocyte infiltration (Macêdo et al., 2020). Consequently, the variations of cytoskeletal proteins

494 indicated that this contamination mixture caused cellular damage in the hepatocytes as previously
495 suggested in the literature (Hadi & Alwan, 2012; Mela et al., 2007).

496 On the other hand, mixture 3 including contamination in Hg, Zn, Ni, Pb induced upregulation
497 of pathways involved in chromosome organization, protein catabolism and protein folding.
498 Chromosomal abnormalities and DNA damage are known effects of heavy metal pollutants (Järup,
499 2003; Parveen & Shadab, 2012; Whitfield & Elliott, 2002), which can lead to abnormalities in cell
500 behaviour during mitotic division and reproductive system in fish (Çavaş & Ergene-Gözükara, 2003;
501 Ebrahimi & Taherianfard, 2011). In our case, mixture 3 seemed to specifically impact telomeres
502 structure, which are repeated sequences of non-coding DNA at the ends of chromosomes and play
503 an important role in stabilizing and protecting coding sequences in eukaryote genomes (Blackburn,
504 1991). These results are in accordance with a previous article which highlighted that some inorganic
505 contaminant (e.g. As, Pb, Cr) seem to cause telomere shortening and others telomere elongation
506 (Kahl & da Silva, 2021; H. Li et al., 2012). Short telomere length is strongly associated with increased
507 mortality and age-related disease risk (Zglinicki & Martin-Ruiz, 2005) and shorter life time expectancy
508 compared to individuals with longer telomere length (Pauliny et al., 2006; Salomons et al., 2009; Vera
509 et al., 2012). Future research on fish response to trace element stress should then consider the
510 assessment of telomere length and telomerase activity. Such effect is likely to be caused by oxidative
511 stress (Epel et al., 2004), either by reactive oxygen species (ROS) generation (by redox-active metals)
512 or by reducing antioxidants (redox-inactive metals) (Koivula & Eeva, 2010). This would explain the
513 over-expression of thioredoxin-like protein, which is believed to serve as a cellular antioxidant by
514 reducing protein disulfide bonds produced by various oxidants such as metals (Hu et al., 2005).
515 Simultaneously trace metal stress activated overexpression of DNA damage repair proteins and
516 chaperone proteins to encounter cellular damages (Table S2). Indeed, another potential biomarker in
517 response to mixture 2 is a component of chaperonin-containing T-complex (TriC) that assists the
518 folding of proteins and participate in telomere maintenance. This protein was also dysregulated in
519 the golden clam (*Corbicula fluminea*) in response to water contamination (Bebianno et al., 2016).

520 Moreover, upregulation of protein catabolism pathway suggests that proteolysis might be activated
521 to remove metal-damaged proteins. Altogether, these regulations could be seen as an early response
522 due to the presence of some trace elements and it underlines the implication of the liver in
523 detoxification processes.

524 Finally, we highlighted that metal contamination level represents a stressor for gilthead
525 seabream. Our results indicate that wild *S.aurata* may be vulnerable to telomere attrition, alterations
526 in redox status and cytoskeleton disorganization in liver as a result of pollution and during juvenile
527 phase. As seabreams mainly store lipids in the liver (McClelland et al., 1995), alteration of this key
528 organ could reduce their chance of survival for their first winter in open water.

529 Muscle proteome response

530 Only mixtures 1 and 2 displayed significant impacts on red muscle proteome. Both mixtures
531 caused an up-regulation of multiple pathways involved in cellular organization and protein
532 localization. This highlights similarities in the process involved, displaying for some of them opposite
533 responses for both tissues. Here again, our results showed that metal stress would reorganize the
534 biological structure of cells which seemed to affect muscle development and contraction. In fact,
535 among the hub proteins affected, ryanodine receptor 1 is an intracellular Ca^{2+} release channel that
536 mediates excitation-contraction coupling in skeletal muscle (Zalk et al., 2015), which also explain the
537 enrichment in the “response to calcium ion” pathway. The disturbance of these pathways suggest
538 that these trace elements are likely to affect muscle function in *S.aurata*, which could result in
539 limitation of seabream juvenile movement.

540 It has been reported that exposure to some environmental pollutants can cause impairment
541 in energy homeostasis and energy allocation (Epelboin et al., 2015; Gardon et al., 2018; Li et al.,
542 2021). Our enrichment analysis results highlighted that mixtures 1 and 2 triggered a general up-
543 regulation of energy metabolism pathways. Carbohydrate metabolism seemed to be particularly
544 affected, as 4 of the 5 hub proteins selected were involved in this process. Particularly, fructose 1,6-
545 biphosphatase, a key enzyme in carbohydrate metabolism also reported as impacted by metal

546 contamination in previous work (Y. Li et al., 2020; Sabir et al., 2019). Interestingly, we identified one
547 protein, which was activated by metal stress and was related to all previous affected pathways. Beta-
548 enolase protein is found in skeletal muscle cells where it has known role in glycolysis and
549 gluconeogenesis (Butterfield & Lange, 2009), but also may play a role in muscle development and
550 regeneration (Merkulova et al., 2000). We suggest that beta enolase may be an enzyme of choice for
551 assessing myocyte response to metal stress. The over-expression of proteins involved in
552 gluconeogenesis might reflect an inefficient foraging and/or help to increase the balance of glucose
553 and maintain the energy demand for the organisms under trace metal stress (such as cytoskeleton
554 remodeling). However, more energy allocated in some specific aspects would lead to the shortage
555 of others (energy trade-off, Stearns, 1989), such as growth or reproduction (Wood et al., 2011). An
556 energy trade-off could also explain the general down-regulation of translation in response to mixture
557 2. In eukaryotic cells, ribosome production indeed represents one of the most-energy consuming
558 process, which adapts to changes in intracellular energy status (Murayama et al., 2008). Monitoring
559 daily growth rates and reproductive investment of individuals with differential metal burden would
560 help to identify the potential trade-offs that occur for this species in a challenging contaminated
561 area. Reading daily increments of otolith may also allow rebuilding growth rate a posteriori and
562 should deserve further investigation in the future of seabream monitoring (Kruitwagen et al., 2006).

563 Conclusion

564 The present study highlighted both the extent of trace element accumulation in juveniles of
565 gilthead seabreams in the Gulf of Lions and its effect on fish physiology. Results revealed differential
566 contamination pattern between lagoons, which might lead to contrasted quality as nurseries for
567 juveniles of numerous highly prized fish species in addition to seabreams (Brusle & Cambrony, 1992;
568 Quignard et al., 1984; Tournois et al., 2017). Moreover, we highlighted that proteomic signatures
569 provide a powerful discriminator of metal contamination in biomonitoring and holds potential the
570 classification of contaminated areas or fish populations. Checking the validity of the potential
571 biomarkers highlighted here by their targeted analysis in larger cohorts and/or other marine species

572 would improve our ability to better monitor trace element pollution. By analysing the effects of
573 multiple elements simultaneously, our study improves resolution over modular studies of individual
574 contaminants, which may lack biological significance, since contaminants do not exist in isolation
575 (Escher et al., 2020). Because the proteome of the most contaminated fishes was altered while their
576 general condition factor was not, we can suppose that these alterations may be an early indicator of
577 adverse effects that can potentially translate into population relevant outcomes. The results of this
578 study—and particularly the complex changes in protein expression—demonstrate the need for
579 future studies to test for simultaneous effects of multiple concomitant stressors in both controlled
580 condition and in the wild.

581 Acknowledgement

582 We deeply thank Rémi Villeneuve, Olivier Derridj and Jean-Hervé Bourdeix for the logistical support
583 in the field. The authors are grateful to local fishermen for their help in collecting seabreams. This
584 work is part of the project ICIPOP granted by the “Agence Francaise de Developpement” (AFD). A. B.
585 has a PhD grant from University of Montpellier – GAIA doctoral school.

586 References

- 587 Andral, B., & Tomasino, C. (2010). *RINBIO 2009 - Evaluation de la qualité des eaux basée sur l'utilisation de stations*
588 *artificielles de moules en Méditerranée : résultats de la campagne 2009*. 88.
589 <http://archimer.ifremer.fr/doc/00028/13913/>
- 590 Apraiz, I., Mi, J., & Cristobal, S. (2006). Identification of proteomic signatures of exposure to marine pollutants in mussels
591 (*Mytilus edulis*). *Molecular and Cellular Proteomics*, 5(7), 1274–1285. [https://doi.org/10.1074/mcp.M500333-](https://doi.org/10.1074/mcp.M500333-MCP200)
592 [MCP200](https://doi.org/10.1074/mcp.M500333-MCP200)
- 593 Aslam, S., & Yousafzai, A. M. (2017). Chromium toxicity in fish: A review article. ~ 1483 ~ *Journal of Entomology and Zoology*
594 *Studies*, 5(3), 1483–1488.
- 595 Audouin, J. (1962). La daurade de l'étang de Thau (Linné). *Revue Des Travaux de l'Institut Des Peches Maritimes*, 26(1), 105–
596 126.
- 597 Authman, M. M. N. (2011). Environmental and experimental studies of aluminium toxicity on the liver of oreochromis
598 niloticus (Linnaeus, 1757) fish. *Life Science Journal*, 8(4), 764–776.
- 599 Bauer, N. C., Doetsch, P. W., & Corbett, A. H. (2015). Mechanisms Regulating Protein Localization. In *Traffic* (Vol. 16, Issue
600 10, pp. 1039–1061). <https://doi.org/10.1111/tra.12310>
- 601 Bebianno, M. J., Sroda, S., Gomes, T., Chan, P., Bonnafe, E., Budzinski, H., & Geret, F. (2016). Proteomic changes in *Corbicula*
602 *fluminea* exposed to wastewater from a psychiatric hospital. *Environmental Science and Pollution Research*, 23(6),
603 5046–5055. <https://doi.org/10.1007/s11356-015-5395-5>
- 604 Benninghoff, A. D. (2007). Toxicoproteomics - The next step in the evolution of environmental biomarkers? *Toxicological*
605 *Sciences*, 95(1), 1–4. <https://doi.org/10.1093/toxsci/kfl157>
- 606 Bindea, G., Mlecnik, B., Hackl, H., Charoentong, P., Tosolini, M., Kirilovsky, A., Fridman, W.-H., Pagès, F., Trajanoski, Z., &

- 607 Galon, J. (2009). ClueGO: a Cytoscape plug-in to decipher functionally grouped gene ontology and pathway
608 annotation networks. *Bioinformatics*, 25(8), 1091–1093. <https://doi.org/10.1093/bioinformatics/btp101>
- 609 Blackburn, E. H. (1991). Structure and function of telomeres. *Nature*, 350(6319), 569–573.
610 <https://doi.org/10.1038/350569a0>
- 611 Blewett, T. A., & Leonard, E. M. (2017). Mechanisms of nickel toxicity to fish and invertebrates in marine and estuarine
612 waters. *Environmental Pollution*, 223, 311–322. <https://doi.org/10.1016/j.envpol.2017.01.028>
- 613 Bouchoucha, M., Chekri, R., Leufroy, A., Jitaru, P., Millour, S., Marchond, N., Chafey, C., Testu, C., Zinck, J., Cresson, P.,
614 Mirallès, F., Mahe, A., Arnich, N., Sanaa, M., Bemrah, N., & Guérin, T. (2019). Trace element contamination in fish
615 impacted by bauxite red mud disposal in the Cassidaigne canyon (NW French Mediterranean). *Science of the Total
616 Environment*, 690, 16–26. <https://doi.org/10.1016/j.scitotenv.2019.06.474>
- 617 Braasch, I., Gehrke, A. R., Smith, J. J., Kawasaki, K., Manousaki, T., Pasquier, J., Amores, A., Desvignes, T., Batzel, P., Catchen,
618 J., Berlin, A. M., Campbell, M. S., Barrell, D., Martin, K. J., Mulley, J. F., Ravi, V., Lee, A. P., Nakamura, T., Chalopin, D.,
619 ... Postlethwait, J. H. (2016). The spotted gar genome illuminates vertebrate evolution and facilitates human-teleost
620 comparisons. *Nature Genetics*, 48(4), 427–437. <https://doi.org/10.1038/ng.3526>
- 621 Brusle, J., & Cambrony, M. (1992). Les lagunes Méditerranéennes: des nurseries favorables aux juvéniles de poissons
622 euryhalins et/ou des pièges redoutables pour eux? *Vie et Milieu*, 42(2), 193–205.
- 623 Butterfield, D. A., & Lange, M. L. B. (2009). Multifunctional roles of enolase in Alzheimer's disease brain: Beyond altered
624 glucose metabolism. *Journal of Neurochemistry*, 111(4), 915–933. <https://doi.org/10.1111/j.1471-4159.2009.06397.x>
- 625 Canli, M., & Atli, G. (2003). The relationships between heavy metal (Cd, Cr, Cu, Fe, Pb, Zn) levels and the size of six
626 Mediterranean fish species. *Environmental Pollution*, 121(1), 129–136. [https://doi.org/10.1016/S0269-7491\(02\)00194-X](https://doi.org/10.1016/S0269-7491(02)00194-X)
- 628 Carapito, C., Burel, A., Guterl, P., Walter, A., Varrier, F., Bertile, F., & Van Dorsselaer, A. (2014). MSDA, a proteomics
629 software suite for in-depth Mass Spectrometry Data Analysis using grid computing. *Proteomics*, 14(9), 1014–1019.
630 <https://doi.org/10.1002/pmic.201300415>
- 631 Çavaş, T., & Ergene-Gözükara, S. (2003). Micronuclei, nuclear lesions and interphase silver-stained nucleolar organizer
632 regions (AgNORs) as cyto-genotoxicity indicators in *Oreochromis niloticus* exposed to textile mill effluent. *Mutation
633 Research - Genetic Toxicology and Environmental Mutagenesis*, 538(1–2), 81–91. [https://doi.org/10.1016/S1383-5718\(03\)00091-3](https://doi.org/10.1016/S1383-5718(03)00091-3)
- 635 Celander, M. C. (2011). Cocktail effects on biomarker responses in fish. *Aquatic Toxicology*, 105(3–4), 72–77.
636 <https://doi.org/10.1016/j.aquatox.2011.06.002>
- 637 Cox, J., Hein, M. Y., Luber, C. A., Paron, I., Nagaraj, N., & Mann, M. (2014). Accurate proteome-wide label-free quantification
638 by delayed normalization and maximal peptide ratio extraction, termed MaxLFQ. *Molecular and Cellular Proteomics*,
639 13(9), 2513–2526. <https://doi.org/10.1074/mcp.M113.031591>
- 640 Cresson, P., Bouchoucha, M., Miralles, F., Elleboode, R., Mahé, K., Maruscak, N., Thebault, H., & Cossa, D. (2015). Are red
641 mullet efficient as bio-indicators of mercury contamination ? A case study from the French Mediterranean. *Marine
642 Pollution Bulletin*, 91(1), 191–199. <https://doi.org/10.1016/j.marpolbul.2014.12.005>
- 643 Cresson, Pierre, Travers-Trolet, M., Rouquette, M., Timmerman, C. A., Giraldo, C., Lefebvre, S., & Ernande, B. (2017).
644 Underestimation of chemical contamination in marine fish muscle tissue can be reduced by considering variable
645 wet:dry weight ratios. *Marine Pollution Bulletin*, 123(1–2), 279–285.
646 <https://doi.org/10.1016/j.marpolbul.2017.08.046>
- 647 DeLorenzo, M. E., & Fleming, J. (2008). Individual and mixture effects of selected pharmaceuticals and personal care
648 products on the marine phytoplankton species *Dunaliella tertiolecta*. *Archives of Environmental Contamination and
649 Toxicology*, 54(2), 203–210. <https://doi.org/10.1007/s00244-007-9032-2>
- 650 Denslow, N. D., Knoebl, I., & Larkin, P. (2005). Chapter 3 Approaches in proteomics and genomics for eco-toxicology.
651 *Biochemistry and Molecular Biology of Fishes*, 6(C), 85–116. [https://doi.org/10.1016/S1873-0140\(05\)80006-2](https://doi.org/10.1016/S1873-0140(05)80006-2)
- 652 Dixon, G. B., Davies, S. W., Aglyamova, G. A., Meyer, E., Bay, L. K., & Matz, M. V. (2015). Genomic determinants of coral heat
653 tolerance across latitudes. *Science*, 348(6242), 1460–1462. <https://doi.org/10.1126/science.1261224>
- 654 Downs, C. A., Richmond, R. H., Mendiola, W. J., Rougée, L., & Ostrander, G. K. (2006). Cellular physiological effects of the
655 MV Kyowa Violet fuel-oil spill on the hard coral, *Porites lobata*. *Environmental Toxicology and Chemistry*, 25(12),
656 3171–3180. <https://doi.org/10.1897/05-509R1.1>

- 657 Ebrahimi, M., & Taherianfard, M. (2011). The effects of heavy metals exposure on reproductive systems of cyprinid fish
658 from Kor River. *Iranian Journal of Fisheries Sciences*, 10(1), 13–24.
- 659 Eisler, R. (2010). Chapter 3 - fishes. In *Compendium of Trace Metals and Marine Biota* (pp. 39–220).
- 660 Endo, T., Hisamichi, Y., Haraguchi, K., Kato, Y., Ohta, C., & Koga, N. (2008). Hg, Zn and Cu levels in the muscle and liver of
661 tiger sharks (*Galeocerdo cuvier*) from the coast of Ishigaki Island, Japan: Relationship between metal concentrations
662 and body length. *Marine Pollution Bulletin*, 56(10), 1774–1780. <https://doi.org/10.1016/j.marpolbul.2008.06.003>
- 663 Epel, E. S., Blackburn, E. H., Lin, J., Dhabhar, F. S., Adler, N. E., Morrow, J. D., & Cawthon, R. M. (2004). Accelerated telomere
664 shortening in response to life stress. *Proceedings of the National Academy of Sciences of the United States of
665 America*, 101(49), 17312–17315. <https://doi.org/10.1073/pnas.0407162101>
- 666 Epelboin, Y., Quéré, C., Pernet, F., Pichereau, V., & Corporeau, C. (2015). Energy and Antioxidant Responses of Pacific Oyster
667 Exposed to Trace Levels of Pesticides. *Chemical Research in Toxicology*, 28(9), 1831–1841.
668 <https://doi.org/10.1021/acs.chemrestox.5b00269>
- 669 Escher, B. I., Stapleton, H. M., & Schymanski, E. L. (2020). Tracking complex mixtures of chemicals in our changing
670 environment. *Science*, 367(6476), 388–392. <https://doi.org/10.1126/science.aay6636>
- 671 Exley, C., Chappell, J. S., & Birchall, J. D. (1991). A mechanism for acute aluminium toxicity in fish. *Journal of Theoretical
672 Biology*, 151(3), 417–428. [https://doi.org/10.1016/S0022-5193\(05\)80389-3](https://doi.org/10.1016/S0022-5193(05)80389-3)
- 673 Farkas, A., Salánki, J., & Specziár, A. (2003). Age- and size-specific patterns of heavy metals in the organs of freshwater fish
674 *Abramis brama* L. populating a low-contaminated site. *Water Research*, 37(5), 959–964.
675 [https://doi.org/10.1016/S0043-1354\(02\)00447-5](https://doi.org/10.1016/S0043-1354(02)00447-5)
- 676 Farrugio, H., Le Corre, G., & Vaudo, G. (1994). *Population dynamics of sea bass, sea-bream and sole exploited by the French
677 multigears demersal fishery in the Gulf of Lions (Northwestern Mediterranean)*.
678 <https://doi.org/10.13140/RG.2.2.27921.99683>
- 679 Fey, P., Bustamante, P., Bosserelle, P., Espiau, B., Malau, A., Mercader, M., Wafo, E., & Letourneur, Y. (2019). Does trophic
680 level drive organic and metallic contamination in coral reef organisms? *Science of The Total Environment*, 667, 208–
681 221. <https://doi.org/10.1016/j.scitotenv.2019.02.311>
- 682 Franco, A., Torricelli, P., & Franzoi, P. (2009). A habitat-specific fish-based approach to assess the ecological status of
683 Mediterranean coastal lagoons. *Marine Pollution Bulletin*, 58(11), 1704–1717.
684 <https://doi.org/10.1016/j.marpolbul.2009.06.016>
- 685 Gaetke, L. M., & Chow, C. K. (2003). Copper toxicity, oxidative stress, and antioxidant nutrients. In *Toxicology* (Vol. 189,
686 Issues 1–2, pp. 147–163). [https://doi.org/10.1016/S0300-483X\(03\)00159-8](https://doi.org/10.1016/S0300-483X(03)00159-8)
- 687 Gardon, T., Reisser, C., Soyez, C., Quillien, V., & Le Moullac, G. (2018). Microplastics Affect Energy Balance and
688 Gametogenesis in the Pearl Oyster *Pinctada margaritifera*. *Environmental Science and Technology*, 52(9), 5277–5286.
689 <https://doi.org/10.1021/acs.est.8b00168>
- 690 Genchi, G., Carocci, A., Lauria, G., Sinicropi, M. S., & Catalano, A. (2021). Thallium Use, Toxicity, and Detoxification Therapy:
691 An Overview. *Applied Sciences*, 11(18), 8322. <https://doi.org/10.3390/app11188322>
- 692 Gobert, S., Pasqualini, V., Dijoux, J., Lejeune, P., Durieux, E. D. H., & Marengo, M. (2017). Trace element concentrations in
693 the apex predator sword fish (*Xiphias gladius*) from a Mediterranean fishery and risk assessment for consumers.
694 *Marine Pollution Bulletin*, 120(1–2), 364–369. <https://doi.org/10.1016/j.marpolbul.2017.05.029>
- 695 Goodson, H. V., & Hawse, W. F. (2002). Molecular evolution of the actin family. *Journal of Cell Science*, 115(13), 2619–2622.
696 <https://doi.org/10.1242/jcs.115.13.2619>
- 697 Grouhel, A., Chiffolleau, J.-F., Crochet, S., Ouisse, V., Galgani, F., & Munaron, D. (2018). *Contamination chimique des
698 sédiments des lagunes méditerranéennes françaises*. <https://doi.org/https://doi.org/10.13155/57885>
- 699 Guérin, T., Chekri, R., Vastel, C., Sirot, V., Volatier, J. L., Leblanc, J. C., & Noël, L. (2011). Determination of 20 trace elements
700 in fish and other seafood from the French market. *Food Chemistry*, 127(3), 934–942.
701 <https://doi.org/10.1016/j.foodchem.2011.01.061>
- 702 Hadi, A. A., & Alwan, S. F. (2012). Histopathological changes in gills, liver and kidney of fresh water fish, *Tilapia zillii*,
703 exposed to aluminum. *International Journal of Pharmacy & Life Sciences*, 3(11), 2071–2081.
- 704 Halliwell, B., & Gutteridge, J. M. C. (2015). *Free Radicals in Biology and Medicine*. Oxford University Press.
705 <https://doi.org/10.1093/acprof:oso/9780198717478.001.0001>

- 706 Hu, P., Brodie, E. L., Suzuki, Y., McAdams, H. H., & Andersen, G. L. (2005). Whole-genome transcriptional analysis of heavy
707 metal stresses in *Caulobacter crescentus*. *Journal of Bacteriology*, *187*(24), 8437–8449.
708 <https://doi.org/10.1128/JB.187.24.8437-8449.2005>
- 709 Isani, G., Andreani, G., Cocchioni, F., Fedeli, D., Carpené, E., & Falcioni, G. (2009). Cadmium accumulation and biochemical
710 responses in *Sparus aurata* following sub-lethal Cd exposure. *Ecotoxicology and Environmental Safety*, *72*(1), 224–
711 230. <https://doi.org/10.1016/j.ecoenv.2008.04.015>
- 712 Isnard, E., Tournois, J., McKenzie, D. J., Ferraton, F., Bodin, N., Aliaume, C., & Darnaude, A. M. (2015). Getting a good start in
713 life? A comparative analysis of the quality of lagoons as juvenile habitats for the gilthead seabream *Sparus aurata* in
714 the Gulf of Lions. *Estuaries and Coasts*, *38*(6), 1937–1950. <https://doi.org/10.1007/s12237-014-9939-6>
- 715 Järup, L. (2003). Hazards of heavy metal contamination. *British Medical Bulletin*, *68*, 167–182.
716 <https://doi.org/10.1093/bmb/ldg032>
- 717 Javed, M., Ahmad, M. I., Usmani, N., & Ahmad, M. (2017). Multiple biomarker responses (serum biochemistry, oxidative
718 stress, genotoxicity and histopathology) in *Channa punctatus* exposed to heavy metal loaded waste water. *Scientific*
719 *Reports*, *7*(1), 1675. <https://doi.org/10.1038/s41598-017-01749-6>
- 720 Jin, L., Bi, Y., Hu, C., Qu, J., Shen, S., Wang, X., & Tian, Y. (2021). A comparative study of evaluating missing value imputation
721 methods in label-free proteomics. *Scientific Reports*, *11*(1), 1–11. <https://doi.org/10.1038/s41598-021-81279-4>
- 722 Jovičić, K., Lenhardt, M., & Jarić, I. (2015). Importance of Standardized Reporting of Elemental Concentrations in Fish
723 Tissues. In *Human and Ecological Risk Assessment* (Vol. 21, Issue 8, pp. 2170–2173).
724 <https://doi.org/10.1080/10807039.2015.1032885>
- 725 Kahl, V. F. S., & da Silva, J. (2021). Inorganic elements in occupational settings: A review on the effects on telomere length
726 and biology. *Mutation Research/Genetic Toxicology and Environmental Mutagenesis*, *872*(August), 503418.
727 <https://doi.org/10.1016/j.mrgentox.2021.503418>
- 728 Kamunde, C., Clayton, C., & Wood, C. M. (2002). Waterborne vs. dietary copper uptake in rainbow trout and the effects of
729 previous waterborne copper exposure. *American Journal of Physiology - Regulatory Integrative and Comparative*
730 *Physiology*, *283*(1 52-1), 69–78. <https://doi.org/10.1152/ajpregu.00016.2002>
- 731 Kassambara, A., & Mundt, F. (2020). *factoextra: Extract and Visualize the Results of Multivariate Data Analyses*.
732 <http://www.sthda.com/english/rpks/factoextra>
- 733 Koivula, M. J., & Eeva, T. (2010). Metal-related oxidative stress in birds. *Environmental Pollution*, *158*(7), 2359–2370.
734 <https://doi.org/10.1016/j.envpol.2010.03.013>
- 735 Kokla, M., Virtanen, J., Kolehmainen, M., Paananen, J., & Hanhineva, K. (2019). Random forest-based imputation
736 outperforms other methods for imputing LC-MS metabolomics data: A comparative study. *BMC Bioinformatics*, *20*(1),
737 1–11. <https://doi.org/10.1186/s12859-019-3110-0>
- 738 Koya, R. C., Fujita, H., Shimizu, S., Ohtsu, M., Takimoto, M., Tsujimoto, Y., & Kuzumaki, N. (2000). Gelsolin inhibits apoptosis
739 by blocking mitochondrial membrane potential loss and cytochrome c release. *Journal of Biological Chemistry*,
740 *275*(20), 15343–15349. <https://doi.org/10.1074/jbc.275.20.15343>
- 741 Kruitwagen, G., Hecht, T., Pratap, H. B., & Wendelaar Bonga, S. E. (2006). Changes in morphology and growth of the
742 mudskipper (*Periophthalmus argentilineatus*) associated with coastal pollution. *Marine Biology*, *149*(2), 201–211.
743 <https://doi.org/10.1007/s00227-005-0178-z>
- 744 Kumari, B., Kumar, V., Sinha, A. K., Ahsan, J., Ghosh, A. K., Wang, H., & DeBoeck, G. (2017). Toxicology of arsenic in fish and
745 aquatic systems. *Environmental Chemistry Letters*, *15*(1), 43–64. <https://doi.org/10.1007/s10311-016-0588-9>
- 746 Langfelder, P., & Horvath, S. (2008). WGCNA: An R package for weighted correlation network analysis. *BMC Bioinformatics*,
747 *9*. <https://doi.org/10.1186/1471-2105-9-559>
- 748 Laviale, M., Prygiel, J., & Créach, A. (2010). Light modulated toxicity of isoproturon toward natural stream periphyton
749 photosynthesis: A comparison between constant and dynamic light conditions. *Aquatic Toxicology*, *97*(4), 334–342.
750 <https://doi.org/10.1016/j.aquatox.2010.01.004>
- 751 Lê, S., Josse, J., & Husson, F. (2008). FactoMineR: An R package for multivariate analysis. *Journal of Statistical Software*,
752 *25*(1), 1–18. <https://doi.org/10.18637/jss.v025.i01>
- 753 Li, H., Engström, K., Vahter, M., & Broberg, K. (2012). Arsenic exposure through drinking water is associated with longer
754 telomeres in peripheral blood. *Chemical Research in Toxicology*, *25*(11), 2333–2339.
755 <https://doi.org/10.1021/tx300222t>

- 756 Li, Y., & Wang, W. X. (2021). Integrated transcriptomics and proteomics revealed the distinct toxicological effects of multi-
757 metal contamination on oysters. *Environmental Pollution*, 284(June), 117533.
758 <https://doi.org/10.1016/j.envpol.2021.117533>
- 759 Li, Y., Zhang, X., Meng, J., Chen, J., You, X., Shi, Q., & Wang, W. X. (2020). Molecular responses of an estuarine oyster to
760 multiple metal contamination in Southern China revealed by RNA-seq. *Science of the Total Environment*, 701,
761 134648. <https://doi.org/10.1016/j.scitotenv.2019.134648>
- 762 López-Pedrouso, M., Varela, Z., Franco, D., Fernández, J. A., & Aboal, J. R. (2020). Can proteomics contribute to
763 biomonitoring of aquatic pollution? A critical review. *Environmental Pollution*, 267, 115473.
764 <https://doi.org/10.1016/j.envpol.2020.115473>
- 765 Lundberg, E., & Borner, G. H. H. (2019). Spatial proteomics: a powerful discovery tool for cell biology. *Nature Reviews*
766 *Molecular Cell Biology*, 20(5), 285–302. <https://doi.org/10.1038/s41580-018-0094-y>
- 767 Macêdo, A. K. S., Santos, K. P. E. dos, Brighenti, L. S., Windmüller, C. C., Barbosa, F. A. R., Ribeiro, R. I. M. de A., Santos, H. B.
768 dos, & Thomé, R. G. (2020). Histological and molecular changes in gill and liver of fish (*Astyanax lacustris* Lütken,
769 1875) exposed to water from the Doce basin after the rupture of a mining tailings dam in Mariana, MG, Brazil.
770 *Science of the Total Environment*, 735, 139505. <https://doi.org/10.1016/j.scitotenv.2020.139505>
- 771 Marengo, M., Durieux, E. D. H., Ternengo, S., Lejeune, P., Degrange, E., Pasqualini, V., & Gobert, S. (2018). Comparison of
772 elemental composition in two wild and cultured marine fish and potential risks to human health. *Ecotoxicology and*
773 *Environmental Safety*, 158(April), 204–212. <https://doi.org/10.1016/j.ecoenv.2018.04.034>
- 774 McClelland, G., Weber, J., Zwingelstein, G., & Brichon, G. (1995). Lipid composition off tissue and plasma in two
775 mediterranean fishes, the gilt-head sea bream (*Chrysophrys auratus*) and the European seabass (*Dicentrarchus*
776 *labrax*). *Canadian Journal of Fisheries and Aquatic Sciences*, 52(1), 161–170. <https://doi.org/10.1139/f95-016>
- 777 Mela, M., Randi, M. A. F., Ventura, D. F., Carvalho, C. E. V., Pelletier, E., & Oliveira Ribeiro, C. A. (2007). Effects of dietary
778 methylmercury on liver and kidney histology in the neotropical fish *Hoplias malabaricus*. *Ecotoxicology and*
779 *Environmental Safety*, 68(3), 426–435. <https://doi.org/10.1016/j.ecoenv.2006.11.013>
- 780 Merkulova, T., Dehaupas, M., Nevers, M. C., Créminon, C., Alameddine, H., & Keller, A. (2000). Differential modulation of α ,
781 β and γ enolase isoforms in regenerating mouse skeletal muscle. *European Journal of Biochemistry*, 267(12), 3735–
782 3743. <https://doi.org/10.1046/j.1432-1327.2000.01408.x>
- 783 Mille, T., Cresson, P., Chouvelon, T., Bustamante, P., Brach-Papa, C., Sandrine, B., Rozuel, E., & Bouchoucha, M. (2018).
784 Trace metal concentrations in the muscle of seven marine species: Comparison between the Gulf of Lions (North-
785 West Mediterranean Sea) and the Bay of Biscay (North-East Atlantic Ocean). *Marine Pollution Bulletin*, 135(May), 9–
786 16. <https://doi.org/10.1016/j.marpolbul.2018.05.051>
- 787 Minganti, V., Drava, G., Pellegrini, R. De, & Siccardi, C. (2010). Trace elements in farmed and wild gilthead seabream, *Sparus*
788 *aurata*. *Marine Pollution Bulletin*, 60(11), 2022–2025. <https://doi.org/10.1016/j.marpolbul.2010.07.023>
- 789 Minghetti, M., Leaver, M. J., Carpenè, E., & George, S. G. (2008). Copper transporter 1, metallothionein and glutathione
790 reductase genes are differentially expressed in tissues of sea bream (*Sparus aurata*) after exposure to dietary or
791 waterborne copper. *Comparative Biochemistry and Physiology Part C: Toxicology & Pharmacology*, 147(4), 450–459.
792 <https://doi.org/10.1016/j.cbpc.2008.01.014>
- 793 Minghetti, Matteo, Leaver, M. J., & George, S. G. (2010). Multiple Cu-ATPase genes are differentially expressed and
794 transcriptionally regulated by Cu exposure in sea bream, *Sparus aurata*. *Aquatic Toxicology*, 97(1), 23–33.
795 <https://doi.org/10.1016/j.aquatox.2009.11.017>
- 796 Morais, P., Parra, M. P., Baptista, V., Ribeiro, L., Pousão-Ferreira, P., & Teodósio, M. A. (2017). Response of gilthead
797 seabream (*Sparus aurata* L., 1758) larvae to nursery odor cues as described by a new set of behavioral indexes.
798 *Frontiers in Marine Science*, 4(OCT), 1–13. <https://doi.org/10.3389/fmars.2017.00318>
- 799 Morcillo, P., Esteban, M., & Cuesta, A. (2016). Heavy metals produce toxicity, oxidative stress and apoptosis in the marine
800 teleost fish SAF-1 cell line. *Chemosphere*, 144, 225–233. <https://doi.org/10.1016/j.chemosphere.2015.08.020>
- 801 Munaron, D., Hubert, M., Gonzalez, J.-L., Tapie, N., Budzinski, H., Guyomarch, J., & Andral, B. (2013). PEPS LAG : Projet
802 échantillonneurs passifs pour la surveillance de la contamination chimique des lagunes Méditerranéennes. *Ifremer*
803 *Report, Feb 2013*(n°RST.ODE/LER-LR 13-01), 79p.
- 804 Murayama, A., Ohmori, K., Fujimura, A., Minami, H., Yasuzawa-Tanaka, K., Kuroda, T., Oie, S., Daitoku, H., Okuwaki, M.,
805 Nagata, K., Fukamizu, A., Kimura, K., Shimizu, T., & Yanagisawa, J. (2008). Epigenetic Control of rDNA Loci in Response
806 to Intracellular Energy Status. *Cell*, 133(4), 627–639. <https://doi.org/10.1016/j.cell.2008.03.030>

- 807 Paci, G., Caria, J., & Lemke, E. A. (2021). Cargo transport through the nuclear pore complex at a glance. *Journal of Cell*
808 *Science*, 134(2). <https://doi.org/10.1242/jcs.247874>
- 809 Parveen, N., & Shadab, G. G. H. A. (2012). Cytogenetic evaluation of cadmium chloride on *Channa punctatus*. *Journal of*
810 *Environmental Biology*, 33(3), 663–666.
- 811 Pauliny, A., Wagner, R. H., Augustin, J., Szép, T., & Blomqvist, D. (2006). Age-independent telomere length predicts fitness in
812 two bird species. *Molecular Ecology*, 15(6), 1681–1687. <https://doi.org/10.1111/j.1365-294X.2006.02862.x>
- 813 Pereira, S., Pinto, A. L., Cortes, R., Fontainhas-Fernandes, A., Coimbra, A. M., & Monteiro, S. M. (2013). Gill histopathological
814 and oxidative stress evaluation in native fish captured in Portuguese northwestern rivers. *Ecotoxicology and*
815 *Environmental Safety*, 90, 157–166. <https://doi.org/10.1016/j.ecoenv.2012.12.023>
- 816 Perez-Riverol, Y., Csordas, A., Bai, J., Bernal-Llinares, M., Hewapathirana, S., Kundu, D. J., Inuganti, A., Griss, J., Mayer, G.,
817 Eisenacher, M., Pérez, E., Uszkoreit, J., Pfeuffer, J., Sachsenberg, T., Yilmaz, Ş., Tiwary, S., Cox, J., Audain, E., Walzer,
818 M., ... Vizcaíno, J. A. (2019). The PRIDE database and related tools and resources in 2019: Improving support for
819 quantification data. *Nucleic Acids Research*, 47(D1), D442–D450. <https://doi.org/10.1093/nar/gky1106>
- 820 Pyle, G. G., Rajotte, J. W., & Couture, P. (2005). Effects of industrial metals on wild fish populations along a metal
821 contamination gradient. *Ecotoxicology and Environmental Safety*, 61(3), 287–312.
822 <https://doi.org/10.1016/j.ecoenv.2004.09.003>
- 823 Quignard, J. P., Man Wai, R., & Vianet, R. (1984). Les poissons de l'étang de Mauguio (Hérault, France). Inventaire, structure
824 du peuplement, croissance et polymorphisme des tailles. *VIE MILIEU*, 34, 173–183.
825 <https://doi.org/https://hal.sorbonne-universite.fr/hal-03020038>
- 826 Rätz, H. J., & Lloret, J. (2003). Variation in fish condition between Atlantic cod (*Gadus morhua*) stocks, the effect on their
827 productivity and management implications. *Fisheries Research*, 60(2–3), 369–380. [https://doi.org/10.1016/S0165-7836\(02\)00132-7](https://doi.org/10.1016/S0165-7836(02)00132-7)
- 829 Relyea, R. A. (2009). A cocktail of contaminants: How mixtures of pesticides at low concentrations affect aquatic
830 communities. *Oecologia*, 159(2), 363–376. <https://doi.org/10.1007/s00442-008-1213-9>
- 831 Romero, D., Barcala, E., María-Dolores, E., & Muñoz, P. (2020). European eels and heavy metals from the Mar Menor lagoon
832 (SE Spain). *Marine Pollution Bulletin*, 158(June), 111368. <https://doi.org/10.1016/j.marpolbul.2020.111368>
- 833 Sabir, S., Akash, M. S. H., Fiayyaz, F., Saleem, U., Mehmood, M. H., & Rehman, K. (2019). Role of cadmium and arsenic as
834 endocrine disruptors in the metabolism of carbohydrates: Inserting the association into perspectives. *Biomedicine*
835 *and Pharmacotherapy*, 114(December 2018), 108802. <https://doi.org/10.1016/j.biopha.2019.108802>
- 836 Sakuragui, M. M., Paulino, M. G., Pereira, C. D. S., Carvalho, C. S., Sadauskas-Henrique, H., & Fernandes, M. N. (2013).
837 Integrated use of antioxidant enzymes and oxidative damage in two fish species to assess pollution in man-made
838 hydroelectric reservoirs. *Environmental Pollution*, 178, 41–51. <https://doi.org/10.1016/j.envpol.2013.02.032>
- 839 Salomons, H. M., Mulder, G. A., Van De Zande, L., Haussmann, M. F., Linskens, M. H. K., & Verhulst, S. (2009). Telomere
840 shortening and survival in free-living corvids. *Proceedings of the Royal Society B: Biological Sciences*, 276(1670),
841 3157–3165. <https://doi.org/10.1098/rspb.2009.0517>
- 842 Sanchez, B. C., Ralston-Hooper, K., & Sepúlveda, M. S. (2011). Review of recent proteomic applications in aquatic toxicology.
843 *Environmental Toxicology and Chemistry*, 30(2), 274–282. <https://doi.org/10.1002/etc.402>
- 844 Schull, Q., Beauvieux, A., Viblanc, V., Metral, L., Leclerc, L., Romero, D., Pernet, F., Quéré, C., Derolez, V., Munaron, D.,
845 McKindsey, C. W., Saraux, C., & Bourjea, J. (2023). An Integrative Perspective on Fish Health: Environmental and
846 Anthropogenic Pathways Affecting Fish Stress. *Marine Pollution Bulletin*, in press
- 847 Stachowski-Haberkorn, S., Becker, B., Marie, D., Haberkorn, H., Coroller, L., & de la Broise, D. (2008). Impact of Roundup on
848 the marine microbial community, as shown by an in situ microcosm experiment. *Aquatic Toxicology*, 89(4), 232–241.
849 <https://doi.org/10.1016/j.aquatox.2008.07.004>
- 850 Stearns, S. C. (1989). The Evolutionary Significance of Phenotypic Plasticity. *BioScience*, 39(7), 436–445.
851 <https://doi.org/10.2307/1311135>
- 852 Stekhoven, D. J., & Bühlmann, P. (2012). Missforest-Non-parametric missing value imputation for mixed-type data.
853 *Bioinformatics*, 28(1), 112–118. <https://doi.org/10.1093/bioinformatics/btr597>
- 854 Storelli, M. M., Barone, G., Garofalo, R., & Marcotrigiano, G. O. (2007). Metals and organochlorine compounds in eel
855 (*Anguilla anguilla*) from the Lesina lagoon, Adriatic Sea (Italy). *Food Chemistry*, 100(4), 1337–1341.
856 <https://doi.org/10.1016/j.foodchem.2005.10.071>

- 857 Tao, S., Wen, Y., Long, A., Dawson, R., Cao, J., & Xu, F. (2001). Simulation of acid-base condition and copper speciation in the
858 fish gill microenvironment. *Computers and Chemistry*, 25(3), 215–222. <https://doi.org/10.1016/S0097->
859 8485(00)00083-8
- 860 Tournois, J., Darnaude, A. M., Ferraton, F., Aliaume, C., Mercier, L., & McKenzie, D. J. (2017). Lagoon nurseries make a major
861 contribution to adult populations of a highly prized coastal fish. *Limnology and Oceanography*, 62(3), 1219–1233.
862 <https://doi.org/10.1002/lno.10496>
- 863 Treyer, A., & Müsch, A. (2013). Hepatocyte Polarity. In *Comprehensive Physiology* (Vol. 3, Issue 1, pp. 243–287). Wiley.
864 <https://doi.org/10.1002/cphy.c120009>
- 865 Välikangas, T., Suomi, T., & Elo, L. L. (2018). A systematic evaluation of normalization methods in quantitative label-free
866 proteomics. *Briefings in Bioinformatics*, 19(1), 1–11. <https://doi.org/10.1093/bib/bbw095>
- 867 Velasco, A. M., Pérez-Ruzafa, A., Martínez-Paz, J. M., & Marcos, C. (2018). Ecosystem services and main environmental risks
868 in a coastal lagoon (Mar Menor, Murcia, SE Spain): The public perception. *Journal for Nature Conservation*,
869 43(February 2017), 180–189. <https://doi.org/10.1016/j.jnc.2017.11.002>
- 870 Vera, E., Bernardes de Jesus, B., Foronda, M., Flores, J. M., & Blasco, M. A. (2012). The Rate of Increase of Short Telomeres
871 Predicts Longevity in Mammals. *Cell Reports*, 2(4), 732–737. <https://doi.org/10.1016/j.celrep.2012.08.023>
- 872 Verbovsek, T. (2011). A comparison of parameters below the limit of detection in geochemical analyses by substitution
873 methods Primerjava ocenitev parametrov pod mejo določljivosti pri geokemičnih analizah z metodo nadomeščanja.
874 *RMZ – Materials and Geoenvironment*, 58(4), 393–404.
- 875 Whitfield, A. K., & Elliott, M. (2002). Fishes as indicators of environmental and ecological changes within estuaries: A review
876 of progress and some suggestions for the future. *Journal of Fish Biology*, 61(SUPPL. A), 229–250.
877 <https://doi.org/10.1006/jfbi.2002.2079>
- 878 Williams, C. R., & Yoshida-Honmachi, E. P. (2013). Effects of cadmium on olfactory mediated behaviors and molecular
879 biomarkers in coho salmon (*Oncorhynchus kisutch*). *Aquatic Toxicology*, 140–141, 295–302.
880 <https://doi.org/10.1016/j.aquatox.2013.06.010>
- 881 Wood, C. ., Farrell, A. ., & Brauner, C. . (2011). Copper of the Fish Physiology. In *Fish physiology* (pp. 55–133).
- 882 Wood, C. ., Farrell, A. ., & Brauner, C. . (2012). *Homeostasis and Toxicology of Essential Metals*.
- 883 Zalk, R., Clarke, O. B., Georges, A. Des, Grassucci, R. A., Reiken, S., Mancina, F., Hendrickson, W. A., Frank, J., & Marks, A. R.
884 (2015). Structure of a mammalian ryanodine receptor. *Nature*, 517(7532), 44–49.
885 <https://doi.org/10.1038/nature13950>
- 886 Zglinicki, T., & Martin-Ruiz, C. (2005). Telomeres as Biomarkers for Ageing and Age-Related Diseases. *Current Molecular*
887 *Medicine*, 5(2), 197–203. <https://doi.org/10.2174/1566524053586545>
- 888 Zhang, X., Smits, A. H., van Tilburg, G. B., Ovaa, H., Huber, W., & Vermeulen, M. (2018). Proteome-wide identification of
889 ubiquitin interactions using UblA-MS. *Nature Protocols*, 13(3), 530–550. <https://doi.org/10.1038/nprot.2017.147>

890

891

892

893

894

895 Table captions

896 **Table 1.** Main variables that contribute to the first three principal components of the PCA on the 31 individuals
897 selected for proteomic analysis. Each PC represent a contaminant profil/mixture.

898

899 Figure captions

900 **Figure 1.** Biplot of PC1 vs PC2 (a) and PC1 vs PC3 (b) of the PCA built with level of inorganic contaminants
901 present in at least 50% of the 135 sampled juveniles. Each point represents an individual. The larger circles
902 represent the barycentre of the individuals for a given lagoon.

903 **Figure 2.** Biplot of PC1 vs PC2 (a) and PC1 vs PC3 (b) of the PCA built with level of inorganic contaminants
904 present the 31 individuals selected for proteomic analysis. Each point represents an individual. Colours indicate
905 contamination level of individuals (HI: High contamination and LI: Low contamination). The larger circles
906 represent the barycentre of the individuals for a given group.

907 **Figure 3.** Correlations between module eigengenes (columns) and trace element mixtures (rows) for liver (a)
908 and red muscle (b) proteome. Values with module names indicates the number of proteins belonging to each
909 module. Values in the cells are Spearman's correlation coefficients. Blank cells indicate non-significant
910 correlation ($P > 0.05$). *: $P < 0.05$, **: $P < 0.01$

911 **Figure 4.** Significant GO terms (FDR < 0.001) and ontological relationships in liver. Circle size indicates the level
912 of FDR-adjusted statistical significance. Terms enriched in the same module were grouped and presented in the
913 same color. Each leading term, which has the highest significance, is indicated by colored font. Biological
914 processes were grouped in larger pathways (large grey circles).

915 **Figure 5.** Significant GO terms (FDR < 0.001) and ontological relationships in red muscle. Circle size indicates the
916 level of FDR-adjusted statistical significance. Terms enriched in the same module were grouped and presented
917 in the same color. Each leading term, which has the highest significance, is indicated by colored font. Biological
918 processes were grouped in larger pathways (large grey circles).

919 Tables

920

921 **Table 1.**

Mixture 1- PC1		Mixture 2 - PC2		Mixture 3 - PC3	
-	+	-	+	-	+
None	Al, Cu, Sr, Pb, Ni, Cr, Tl, Ti	Pb	Rb, Tl, As, Zn	Sr	Hg, Zn, Ni, Pb

922

923

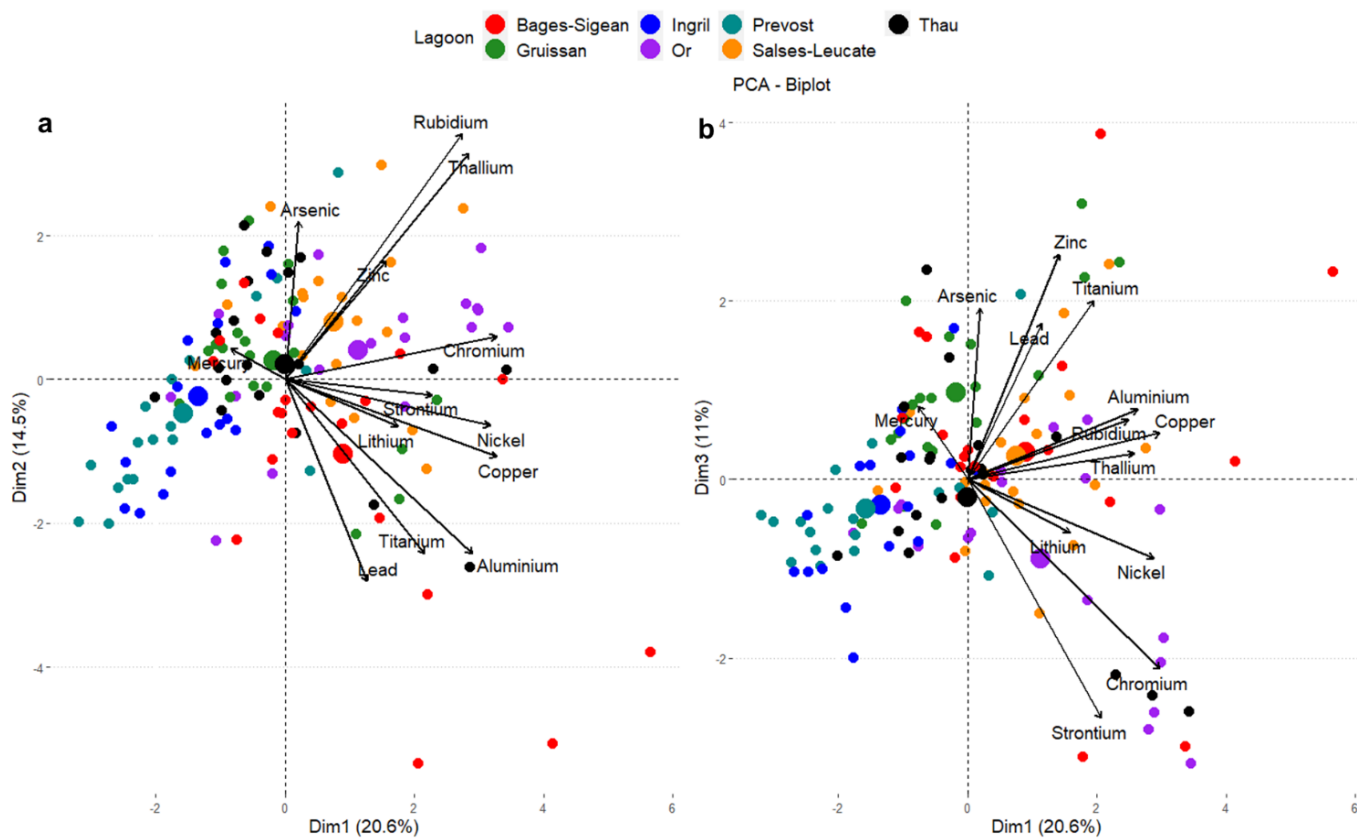
924

925

926

927

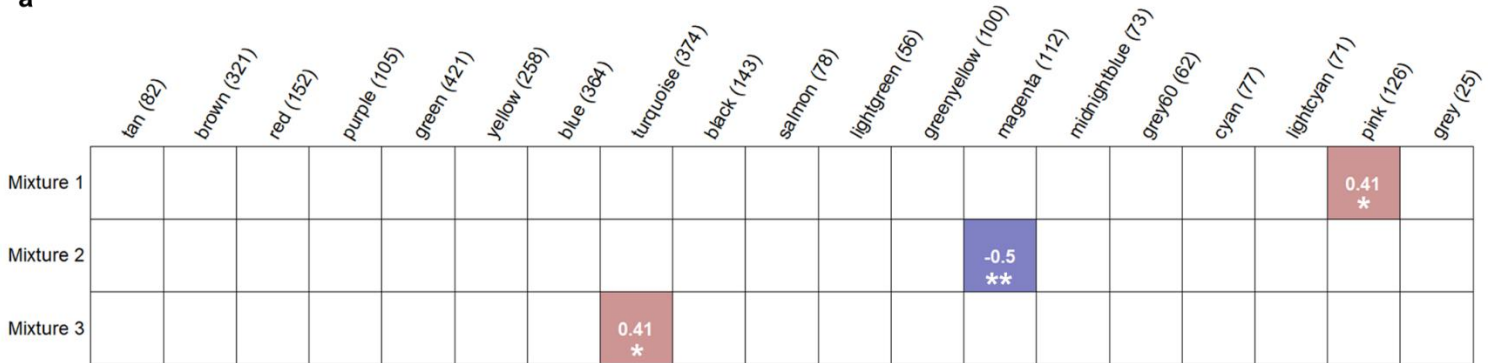
928 Figures



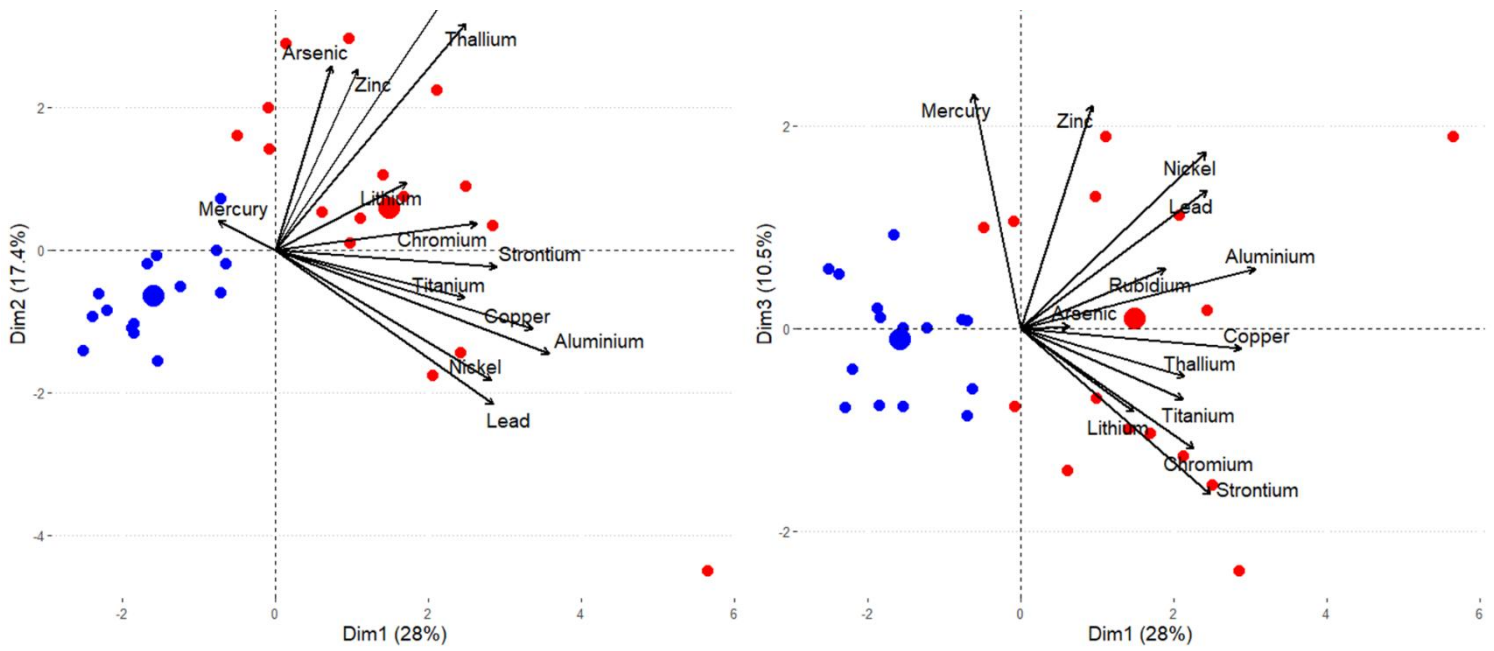
929 **Figure 1.**

930 **Figure 2.**

a



b



931 **Figure 3.**

932

933

934

935

936

937

938

939

940

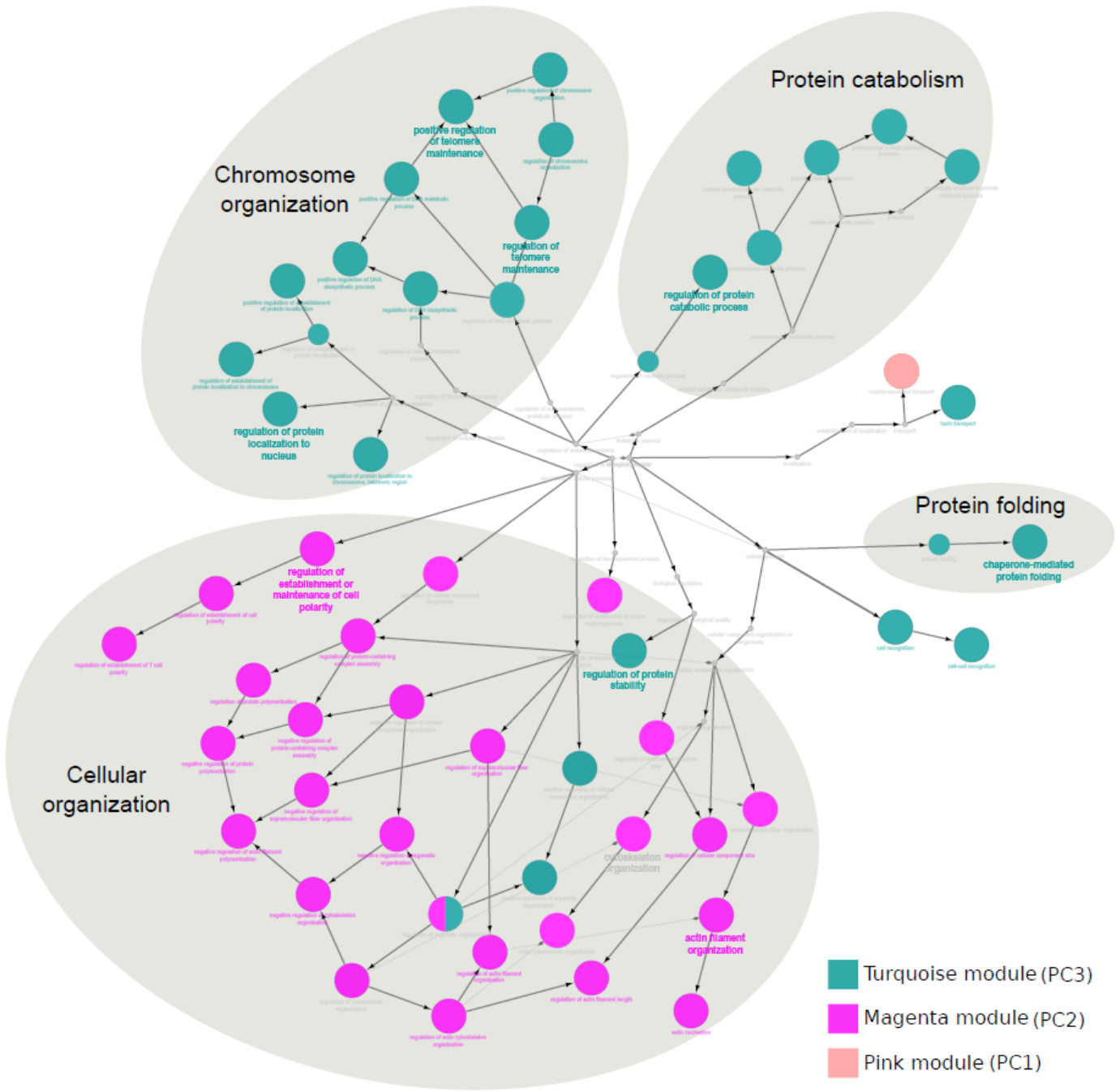
941

942

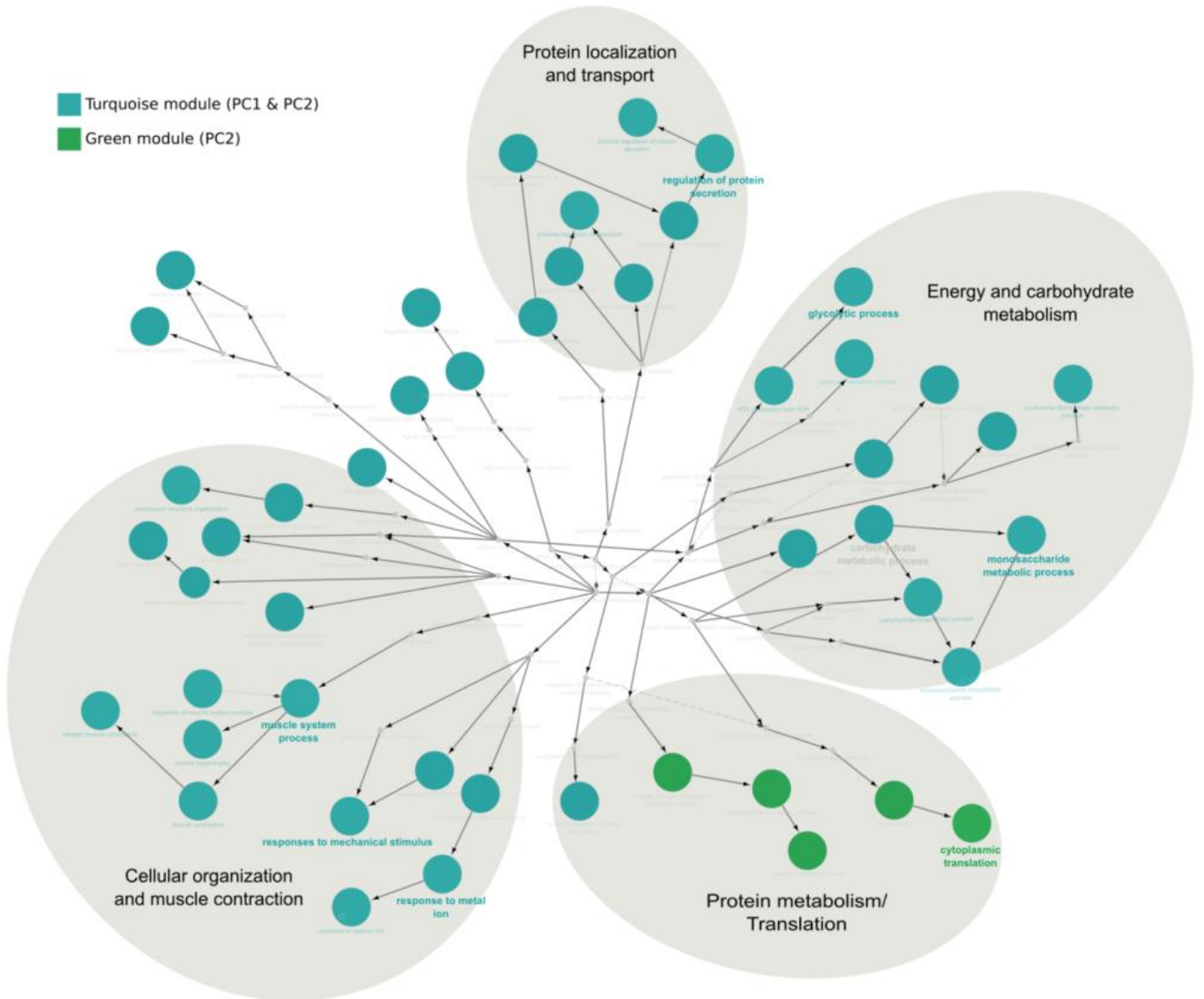
943

944

945



946 **Figure 4.**



947 **Figure 5.**